

Low Temperature Development and Characterization Properties of Mg-Al Spinel by Sol-Gel Process

A thesis submitted in partial fulfilment of the requirement
for the award of the degree

Master of Technology

In

Material Engineering

Submitted By

ALAPAN GHOSH

Exam Roll No: M4MAT22009

Class Roll No: 002011303009

Registration No: 154371 of 2020-21

Under the supervision of

Dr. Sathi Banerjee

Associate Professor,

Dept. of Metallurgical and

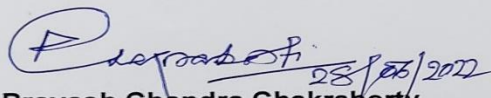
Material Engineering

JADAVPUR UNIVERSITY

Kolkata-700032

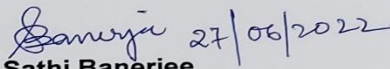
To Whom It may Concern

This is to certify that **Alapan Ghosh** (Exam Roll No: **M4MAT22009**) has completed the thesis "**Low Temperature Development And Characterization Properties of Mg-Al Spinel By Sol Gel Process**" during the academic session 2020-2022 under the supervision of **Dr. Sathi Banerjee**, associate professor, department of Metallurgical and Material Engineering, Jadavpur University, in partial fulfilment of the requirement for the award of the degree of Master of Technology in Material Engineering in the department of Metallurgical and Material Engineering. The work, in our opinion, meets the requirements for which it was submitted. It is also certified that other sources of information have been acknowledged in the thesis.

 28/06/2022

Prof. Pravash Chandra Chakraborty
Head of the Department
Department of Metallurgical
and Material Engineering
Jadavpur University
Kolkata-700032

Head of the Dept.
Metallurgical & Material Engg. Dept.
Jadavpur University
Kolkata-700032

 27/06/2022

Dr. Sathi Banerjee
Associate Professor
Department of Metallurgical and
Material Engineering
Jadavpur University
Kolkata-700032

Associate Professor
Metallurgical & Material Engg. Dept.
Jadavpur University
Kolkata - 700032

 28/06/2022

Prof. Chandan Mazumder
Dean, Faculty of Engineering and Technology
Jadavpur University
Kolkata-700032



DEAN
Faculty of Engineering & Technology
JADAVPUR UNIVERSITY
KOLKATA-700 032

REDMI NOTE 9 PRO

CERTIFICATE OF EXAMINATION

The foregoing thesis is officially authorised as a credible study of an engineering subject that has been carried out and presented in such a way that it can be accepted as a prerequisite for the degree for which it has been submitted. It should be recognised that the undersigned's approval does not necessarily imply that the undersigned endorses any statement made, opinion expressed, or conclusion reached therein, but rather that the thesis was approved only for the purpose for which it was submitted.

Final Examiners for Evaluation of thesis

1.

2.

Date:

Signature of the Examiners

ACKNOWLEDGEMENT

I owe my department a huge debt of gratitude for allowing me to work on this fascinating project. My thesis supervisor, **Dr. Sathi Banerjee** of the Department of Metallurgical and Material Engineering at Jadavpur University in Kolkata, has my heartfelt gratitude. I owe her a debt of gratitude for her earnest assistance and helpful advice during my thesis research. Her constant supervision aided me in completing my tasks more quickly. I'd want to express my gratitude to all of the teachers and staff members for their invaluable assistance and support throughout the project's implementation. I'd want to express my gratitude to **Mr. Sudhir Ghosh** for his unwavering support during laboratory tests. I would like to express my gratitude to **Srinath Ranjan Ghosh**, Research Scholar, Department of Metallurgical and Material Engineering, as well as all of my friends, for their unwavering support during my project. Despite my greatest attempts to maintain correctness and excellence, there are occasional inconsistencies. **Prof. Pravash chandra Chakraborty**, for his gracious cooperation, is greatly appreciated.

Finally, I'd like to express my gratitude to my parents for their unwavering support during my project.

DATE:

ALAPAN GHOSH

| CONTENTS | PAGES |
|--|--------------|
| ABSTRACT | 6 |
| CHAPTER 1 INTRODUCTION | 7 |
| 1. Spinel Group | 8 |
| 1.1. Types Of Spinel | 8 |
| 2.Refractory Materials | 10 |
| 2.1. Types Of Refractories | 11 |
| 2.2. General required properties of refractories | 11 |
| 3.Crystal structure of MgAl ₂ O ₄ spinel | 12 |
| 4.Physical Properties Of MgAl ₂ O ₄ | 13 |
| 5.Phase Diagram Of MgAl ₂ O ₄ | 15 |
| CHAPTER 2 LITERATURE REVIEW | 17 |
| 2.1. MgAl ₂ O ₄ Spinel as a Refractory Material | 18 |
| 2.2. Corrosion of the lining material in contact with slag Process | 18 |
| 2.3. Various Route of Synthesis of MgAl ₂ O ₄ Spinel | 22 |
| 2.4. Selection Of Citric Acid as the fuel agent | 24 |
| 2.5. Microhardness of MgAl ₂ O ₄ spinel | 26 |
| CHAPTER 3 EXPERIMENTAL WORK | 27 |
| 3.1. PREAMBLE | 28 |
| 3.2. SAMPLE PREPARATION | 28 |
| 3.2.1. Preparation Of Solution | 28 |
| 3.2.2. Heating and Drying Of Solution | 28 |
| 3.3. Calcination | 31 |
| 3.4. Hand Grinding Of Calcined Powder | 32 |
| 3.5. Pressing and compacting for microhardness test | 33 |
| 3.6. CURING | 34 |
| 3.7. CHARACTERIZATION: | 37 |
| 3.7.1. DTA/TGA Analysis: | 37 |
| 3.7.2 XRD Analysis | 38 |
| 3.7.3. FTIR Analysis: | 40 |
| 3.7.4. FESEM Analysis | 42 |
| 3.8. Microhardness Testing | 43 |
| CHAPTER 4 RESULT AND DISCUSSION | |
| 4.1. DTA/TGA Analysis | 44 |
| 4.2. XRD Study of Magnesium Aluminate Spinel | 46 |
| 4.3. FTIR | 56 |
| 4.4. FESEM | 57 |
| 4.5. Micro-Hardness- | 60 |
| CHAPTER 5 CONCLUSION AND FUTURE SCOPE | 61 |
| CHAPTER 6 REFERENCES | 65 |

ABSTRACT

A simple, scalable, template free citrate sol-gel technique is used to synthesize layered, agglomerate nano crystal of magnesium aluminium spinel (MgAl_2O_4), a refractory material which is used variety of fields due to its high mechanical strength, as well as its remarkable dielectric and catalytic capabilities. This thesis is concerned about the low temperature synthesis of magnesium aluminate spinel and also this thesis is concerned about the effect of Magnesium Nitrate Hexahydrate ($\text{Mg}(\text{NO}_3)_2 \cdot 6\text{H}_2\text{O}$), Aluminium Nitrate Nonahydrate ($\text{Al}(\text{NO}_3)_3 \cdot 9\text{H}_2\text{O}$) and Citric acid ratio on preparation of spinel. A comparison research among various compositions made using the sol-gel technique is conducted to measure the impact of Magnesium Nitrate Hexahydrate ($\text{Mg}(\text{NO}_3)_2 \cdot 6\text{H}_2\text{O}$), Aluminium Nitrate Nonahydrate ($\text{Al}(\text{NO}_3)_3 \cdot 9\text{H}_2\text{O}$) and Citric acid. The obtained spinel material is characterized by X-ray diffraction, Fourier transform infrared spectroscopy (FTIR) and Field emission scanning electron microscopy (FESEM) to evaluate the particles. Later pellets are formed with compressing of the calcined powder. And microhardness property has been studied. The optimal temperature for the synthesis of MgAl_2O_4 spinel by the citrate sol-gel method is found to be 700°C temperature. Pure nano-sized spinel phase is observed, with a mean particle size of 10-25 nm. The particles are agglomerated and flake like structured, according to morphological analysis. At a greater temperature, a solid state bond forms. And from the microhardness property study It can be said, with increasing citric acid ratio microhardness of the MgAl_2O_4 can be improved.

CHAPTER 1

INTRODUCTION

Magnesium Aluminium spinel $MgAl_2O_4$ is an important functional material. It is member of the larger spinel group of minerals.

1. Spinel Group:

Spinel is a group of minerals with the general formula AB_2X_4 that crystallise in the cubic (isometric) crystal system, with the X anions (typically chalcogens such as oxygen and sulphur) arranged in a cubic close-packed lattice and the cations A and B occupying some or all of the octahedral and tetrahedral sites in the lattice. Although the charges of A and B in the typical spinel structure are +2 and +3 ($A^{2+}B_2^{3+}X_4^{2-}$), other combinations with divalent, trivalent, or tetravalent cation combinations, such as magnesium zinc iron manganese aluminium, chromium, titanium, and silicon, are also possible. Normally, the anion is oxygen.

1.1. Types Of Spinel :

Spinel is a magnesium/aluminum member that belongs to the large spinel group. In the cubic crystal system, it has the formula $MgAl_2O_4$. Its name derives from the word spinella (Latin word), which means spine in reference to its pointed crystals. Spinel, Magnesite, and Chromite were grouped together to form the spinel series. They are usually highly hard minerals with a variety of colours that can be found in carbonate and igneous rocks. Spinel is an appealing subject for material study as well as practical applications. Magnesia alumina spinel is highly refractory and comes in a variety of colours and textures, ranging from opaque to transparent and colourless to blue, brown, and black.

1.1.1. Normal Spinel [20]:

- The simplified form of spinel is AB_2O_4 .
- The cation A^{+2} takes place in tetrahedral sites, while B^{+3} takes place octahedral sites.
- The A-site cations occupy 1/8 of the tetrahedral holes and the B-site cations fill 1/2 of the octahedral holes.
- The classic example belongs to normal spinel of aluminate such as $MgAl_2O_4$, $CoAl_2O_4$, $FeAl_2O_4$ and also ferrite such as $ZnFe_2O_4$, $CdFe_2O_4$.

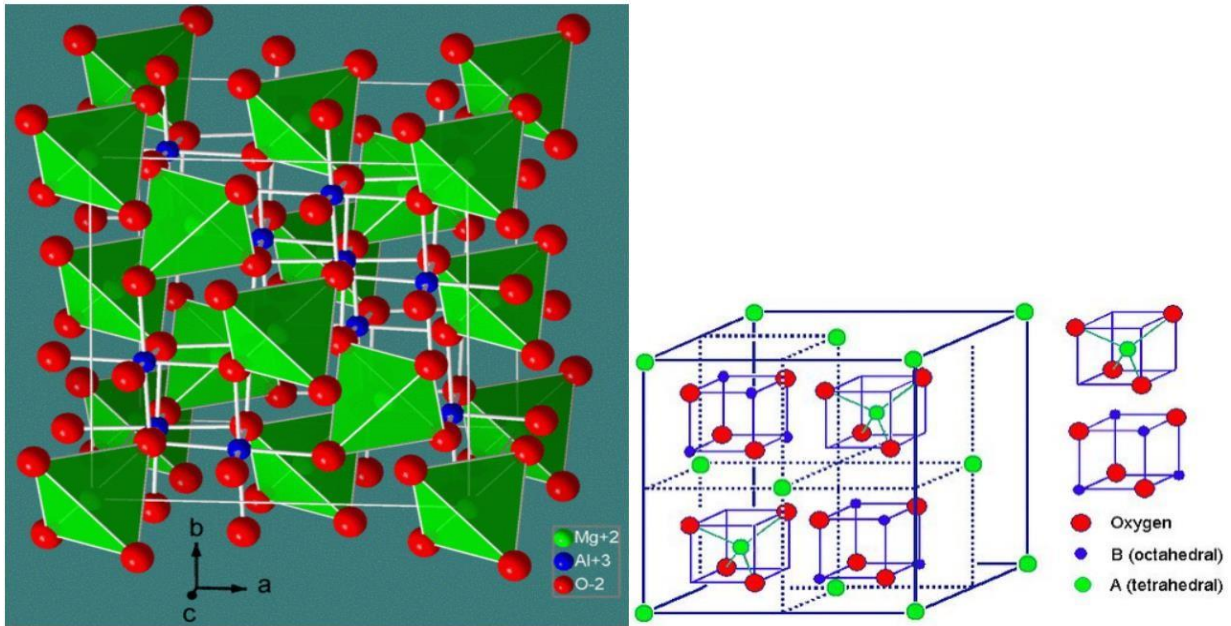


FIG-1.1-A polyhedral view of the normal spinel unit cell is shown at the left, and a simplified view (with the contents of the back half of the cell removed for clarity) is shown above. Each unit cell contains eight formula units and has a composition $A_8B_{16}O_{32}$. [1]

1.1.2. Inverse Spinel[20]:

- Inverse spinel has a similar structure (with the same huge unit cell) in which half of the A-site ions trade places with half of the B-site ions.[2]
- Where the AB ions in parenthesis occupy octahedral positions and the other B ions occupy tetrahedral sites, the typical equation is $B(AB)O_4$. Some spinel and inverse spinel AB combinations are:
 - $A^{2+}B^{3+}$ e.g., $MgAl_2O_4$ (normal spinel)
 - $A^{4+}B^{2+}$ e.g., $Pb_3O_4 = Pb_{II}(Pb_{II}Pb_{IV})O_4$ (inverse spinel)
 - $A^{6+}B^+$, e.g., Na_2WO_4 (normal spinel)
- The majority of ferrites are inverse spinels, such as Fe_3O_4 , $NiFe_2O_4$, and $CoFe_2O_4$.

Magnesium Aluminium Spinel is employed in a variety of fields because of its high temperature refractory qualities, mechanical strength, chemical resistance[3], thermal shock resistance[4], and dielectric and catalytic capabilities[5]. Due to its refractory qualities, it can resist high temperatures; we shall describe these properties here.

2. Refractory Materials:

A refractory material, often known as a refractory, is a substance that can endure extreme heat without softening, melting, or deforming. Polycrystalline, polyphase, inorganic, non-metallic, porous, and heterogeneous are some characteristics of refractories[6].

They are usually made up of oxides, carbides, and nitrides of the following materials: silicon, aluminium, magnesium, calcium, boron, chromium, and zirconium,

The basic functions are,

- They serve as a thermal barrier between a hot medium (such as flue gases, liquid metal, molten slags, or molten salts) and the containing vessel's wall.
- Refractories imply a strong physical protection, preventing the erosion of walls by the circulating hot medium.
- They serve as a corrosion-protective chemical barrier.
- They serve as thermal insulation, ensuring that heat is retained.
- Silicon, aluminium, magnesium, calcium, and zirconium oxides, as well as non-oxide refractories such as carbides, nitrides, borides, silicates, and graphite, are the most common raw materials utilised in the production of refractories.

Due to their high quality features, refractory materials are used in a variety of industrial applications, including the manufacturing of ferrous and non-ferrous metals, cement, glass, ceramics, chemicals, and so on. Refractory materials play a significant role in the following areas.

- furnaces
- kilns
- Boilers
- Incinerators

2.1. Types Of Refractories:

Refractories can be classified in following ways:

On the basis of chemical nature materials:

- Neutral Refractories (Chromite ,Graphite etc)
- Acid Refractories (Alumina silicate, zirconia ,Silica etc)
- Basic Refractories (Frosterite, Dolomite, Magnesite etc)

On the basis of method of manufacturing:

- Unshaped Refractories (includes mortars, castable and other monolithics)
- Shaped Refractories (available in the form of different brick shapes including the oxides and non- oxides systems)

2.2. General required properties of refractories:

The sort of refractory that are used by us, will be determined by the nature of the working environment. The refractory materials, that are used in the iron and steel industry must pass through a rigorous testing process. There are numerous sorts of strict environments, which are detailed here.

- A large quantity of molten metal load
- Refractories must be able to withstand extremely high temperatures, up to 1600°C.
- Slag attack, which is corrosive in nature, can occur.

The ongoing advancement of technology for improved results makes such an operational environment even more challenging. These are some of the ever-changing features:

- Further improvement for innovation and advancement is taking place in metal extraction technologies.
- The operating temperature is rising.
- Challenge of having longer service life

To overcome the aforementioned obstacles, specific properties in the nature of refractory materials are required, and these are detailed below.

1. Refractoriness: It is a feature of a material that allows it to resist high temperatures in operating settings without significant softening. The softening temperature of the material should be higher than the working furnace temperature.
2. Porosity: A material's porosity is the ratio of its pore volume to its bulk volume. Porosity should be low in a good refractory.[7]
3. Thermal spalling: This is the tendency of a refractory brick to fracture, flake, peel, or crack when exposed to high temperatures or rapid temperature changes. Thermal spalling should be minimised in a good refractory.[8]
4. Mechanical Strength: Even at working temperatures, a refractory material should have a high mechanical strength. Under the weight of a heavy load, fire clay bricks will collapse. Silica bricks, a refractory material, have a high load bearing capacity.[6]
5. Chemical inertness: Refractory materials should be chemically inert to slag, fuel, and furnace gases, and other things.[6]
6. Thermal expansion: The thermal expansion of a good refractory should be as small as possible.[9]
7. Electrical conductivity: They should have a low electrical conductivity.

3. Crystal structure of MgAl₂O₄ spinel:

Bragg and Nishikawa [11,12] independently published the crystal structure of MAS (Fig. 1). The spinel structure (also known as the garnet structure) takes its name from the mineral spinel (MgAl₂O₄), which has an AB₂O₄ general composition. The structure of MAS is similar to that of a diamond. The positions of the A ions in the diamond structure are nearly identical to the places occupied by carbon atoms. This could explain why this group has a comparatively high hardness and density. The other ions in the lattice are arranged to match the symmetry of the diamond structure. They do, however, disrupt the cleavage because none of the members of this group have cleavage directions. Mg₈Al₁₆O₃₂ can be written as the unit cell of the 2-3 MAS, in which 32 oxygen anions are face

centred cubic (fcc) close packed with a space group $Fd3m$ (number 227), with eight $MgAl_2O_4$ units per cubic cell. Such close packing provides 64 divalent tetrahedral(IV) coordinated cation sites and 32 octahedral (VI) coordinated trivalent cation sites, of which only 24 are filled.

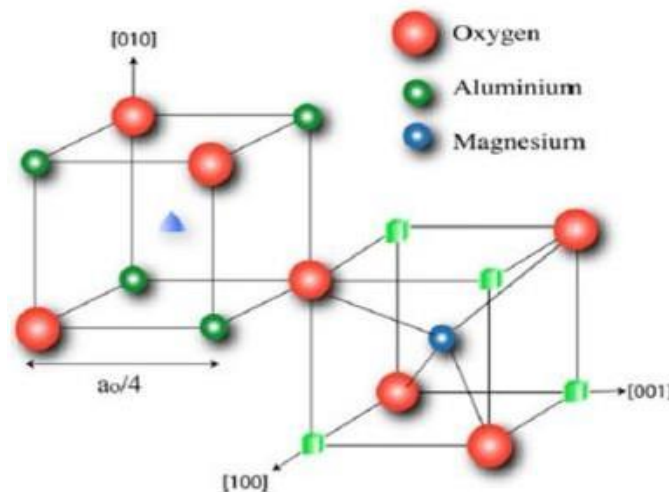


FIG-1.2: Structure of MAS: Mg ions sit at tetrahedral sites while Al ions occupy octahedral sites; unoccupied tetrahedral sites are represented by (blue) triangles and octahedral sites are shown by (green) cubes.

The cations (typically metals) occupy one-eighth of of the tetrahedral sites and half of the octahedral sites in the unit cell. The anion sub-lattice is placed in a pseudo-cubic spatial arrangement that is closely packed. $MgAl_2O_4$ has $Fd3m$ as its space group space and lattice parameter, and 'a' is 8.08435.

4. Physical Properties Of $MgAl_2O_4$:

The followings are some of the physical properties of $MgAl_2O_4$ spinel:

4.1. High Melting Point: As the fusion melting point is $2135^{\circ}C$, it can tolerate a high temperature range. We know that all types of steel have a melting point below $2000^{\circ}C$, thus it can be used as a refractory for steel production.

4.2. Hardness: As $MgAl_2O_4$ spinel is rarely found naturally, it is artificially synthesised. The hardness value measured for nanocrystallite $MgAl_2O_4$ spinel ranged from 2.89 to 7.79 GPa.[13,14]

4.3. High Electric Resistivity: As the energy bandgap is more than 7.5 eV, it has a high electrical resistivity, making it a good refractory material.[14]

4.4. Low Thermal Expansion:

It has relatively low thermal expansion coefficient which is $9 \times 10^{-6} \text{ c}^{-1}$ between 30 and 1400°C .[15]

4.5. Chemically Inertness:

As MgAl_2O_4 has a greater chemical resistance at higher temperatures than standard chromite-based refractories, it has been used in cement rotary kilns and steel ladles.[16,17]

4.6. Mechanical Strength: At room temperature as well as at higher temperatures, it has a high mechanical strength. Its strength varies from 135 MPa to 216 MPa at room temperature, and from 120 MPa to 205 MPa at elevated temperatures (1300° C).[14]

4.7. Density:

MgAl_2O_4 spinel has relatively low density as 3.93gm/cc.[18]

5. Phase Diagram Of $MgAl_2O_4$ [19]:

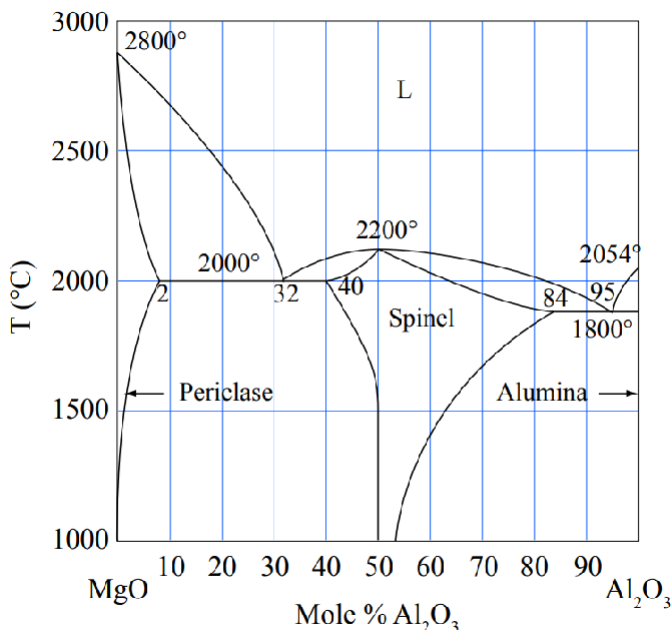
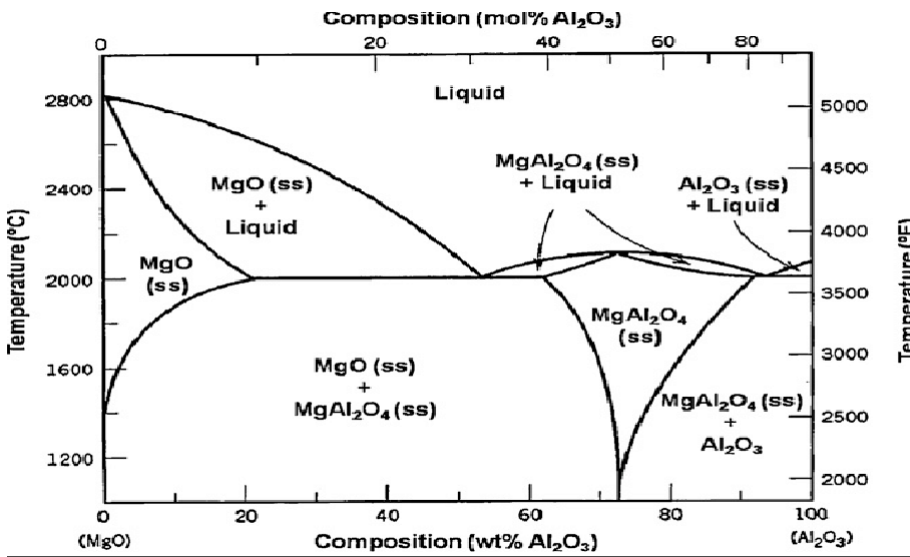


FIG-1.3-PHASE DIAGRAM OF $MgAl_2O_4$

- Pure magnesia has a melting temperature of 2800 $^{\circ}C$.
- Pure alumina has a melting temperature of 2054 $^{\circ}C$.
- Magnesia can be dissolved in 2 percent alumina at 2000 $^{\circ}C$ it is the maximum solubility. Periclase is the solid solution of alumina in magnesia.
- When it comes to the spinel group, magnesium aluminate ($MgAl_2O_4$) is a major figure. The binary system of magnesia and alumina is shown in the phase diagram. The solubility of alumina varies from 40% (at 2000 $^{\circ}C$) to 84% (at 1800 $^{\circ}C$) as seen in the graph. At 2200 $^{\circ}C$, the spinel, which contains 50% alumina, melts.

- At 2200°C, partial solidification of magnesia occurs with an 82 percent magnesia alloy and equal amounts periclase and liquid.
- The cooling of 68 percent magnesia 32 percent alumina alloys from liquid phase to two solid phases occurs at 2000°C. Periclase, which contains 2% alumina, is one of the solid phases, while MgAl_2O_4 , which includes 40% alumina, is the other.
- At 2000°C, 73 percent of alumina was found to be half liquid and half MgAl_2O_4 .
- At 1800°C, phase transformation happens from liquid to two solid phases, one of which is spinel of 84 percent alumina and the other is pure alumina, with a composition of 95 percent alumina alloy.

CHAPTER 2

LITERATURE REVIEW

2.1. MgAl₂O₄ Spinel as a Refractory Material:

A refractory material, often known as a refractory, is a material that resists breakdown due to heat, pressure, or chemical attack while maintaining its strength and form at high temperatures. Polycrystalline, poly-phase, inorganic, non-metallic, porous, and heterogeneous are characteristics of refractory. They are composed of silicon, aluminium, magnesium, calcium, boron, chromium, and zirconium oxides, carbides, and nitrides. In the metallurgical, glassmaking, and ceramic industries, refractories play an essential role [22,23]. Corrosion by steel slags, thermal spalling, oxidation of the carbon layer, abrasion by liquid metal, degradation of strength at high temperatures, and molten steel penetration are the key issues that steel ladle refractories (MgO-C bricks) encounter. Here as a substitute MgAl₂O₄ spinel has been widely used.

2.2. Corrosion of the lining material in contact with slag Process:

The corrosion of the lining material of a ladle in contact with slag occurred during steel refining in a ladle. This takes place due to the following occurrences [24,25,26]. The various corrosion phenomena in refractories are depicted in Fig. 2.1.

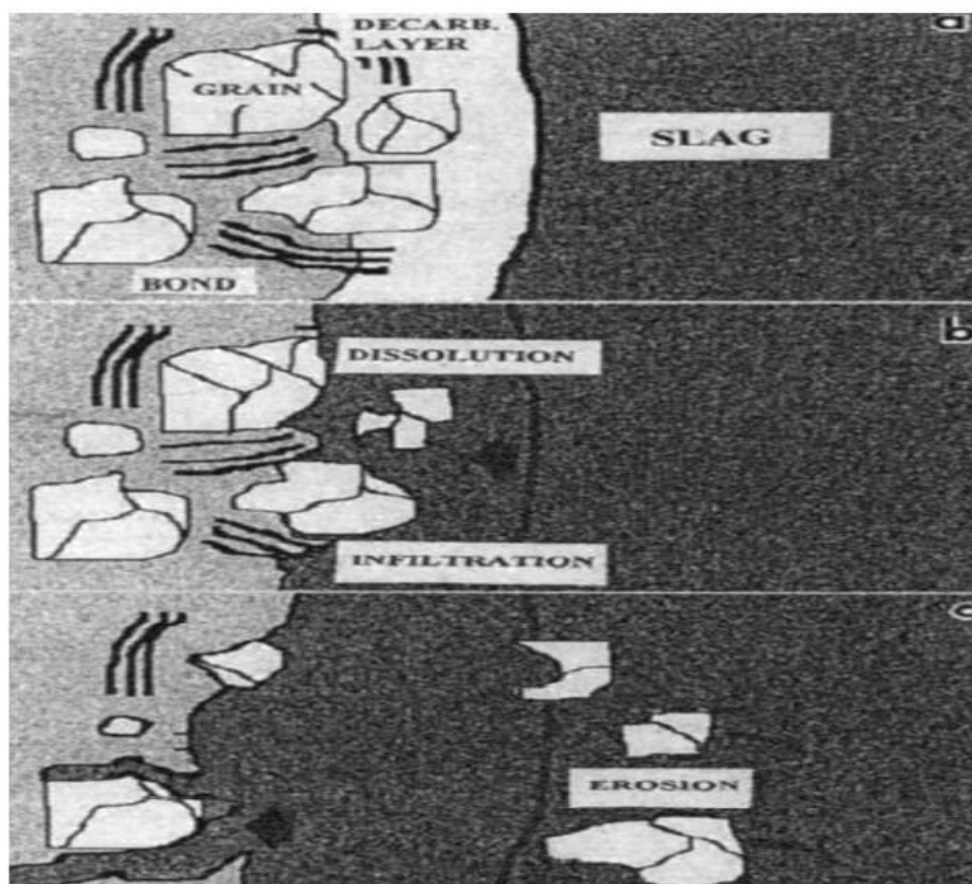


FIG-2.1-CORROSION PHENOMENA OF REFRACTORIES

(i) **Dissolution**- The refractory material was continuously dissolved by the diffusion of reactive species through the liquid slag in a chemical process known as dissolution.

(ii) **Penetration**- Penetration occurs when slag penetrates the pores of the refractory, causing the refractory wall to deteriorate due to differential expansion or contraction between the refractory and the slag.

(iii) **Erosion**- Erosion is a refractory material wear process that is influenced by the viscosity of slag and the velocity of gases that come into contact with the refractory material.

The physical properties of refractory material has been changed as slag particles diffuse into it. The higher wetting angle makes it more difficult for the slag to penetrate into pores and cracks in the refractory [28]. This isn't the only factor that influences infiltration depth. The temperature difference in the brick has an effect on the infiltration depth [28]. Temperature gradients cause the viscosity of slag to increase with increasing distance into the refractory (colder), resulting in a reduction in infiltration depth. Figure 2.2 depicts slag penetration in the refractory as it moves from hot to cold face. The depth of penetration is determined by the refractory's hot face temperature, slag temperature, and viscosity.

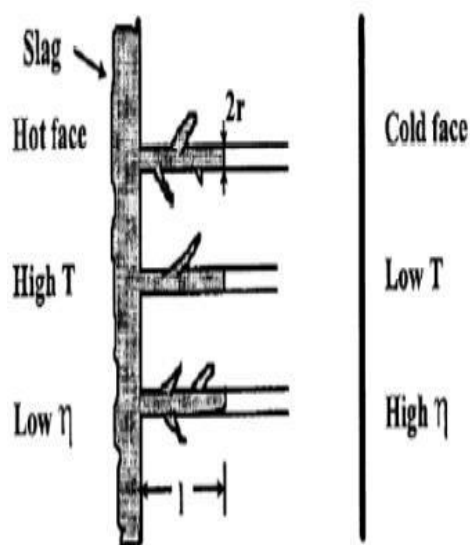


FIG-2.2-SLAG PENETRATION IN THE REFRACTORY AS SLAG MOVES FROM HOT TO COLD FACE

In recent years, nanotechnology has been brought into the field of refractories in order to overcome problems with performance caused by inhomogeneous microstructure. It has been proposed that by enhancing the thermo-chemical characteristics of refractories due to excellent dispersion of nano-sized particles in the matrix of the refractories, the performance of refractories could be significantly improved [29, 30].

Magnesia-spinel refractories developed from pure raw materials with a high degree of direct bonding of MgO-MgO and MgO-spinel grains exhibit high hot temperature strength, enhanced slag resistance, and dimensional stability at high temperatures [31]. Magnesium Nitrate Hexa-hydrate ($\text{Mg}(\text{NO}_3)_2 \cdot 6\text{H}_2\text{O}$) and Aluminium Nitrate Nona-hydrate ($\text{Al}(\text{NO}_3)_3 \cdot 9\text{H}_2\text{O}$) were employed as starting materials in this study to make magnesia-alumina spinel MgAl_2O_4 ceramics.

Magnesium aluminate (MgAl_2O_4) spinel has many industrial applications. The magnesium-aluminate spinel structure also has a number of appealing properties, including high mechanical strength at high temperatures, a high melting point (2135°C), unique optical properties, low expansion at high temperatures, a low dielectric constant, and high chemical inertness and thermal stability [32-33]. It has several applications as a catalyst support [34-38], membranes [39], sensor, dye adsorbent [40], an active component in sensors for humidity measurement [41], and an ideal transparent ceramic based material for arc-enclosing envelopes used at high-temperature [42] due to these properties. This spinel requires excellent purity, small molecule size, high surface area, and consistent pore size distribution for current industrial applications as an adsorbent, catalyst, and catalytic support [34-36], which characteristics are dependent on the preparation processes. The preparation of magnesium aluminate was accomplished using a variety of techniques. Solid-state [43,44], sol-gel [45,46], spray drying [47], pechini technique [48], and co-precipitation [34,49-52] are the most common methods for preparing MgAl_2O_4 spinel.

Although wet-chemical techniques have been successfully employed to create pure spinel nano particles at low temperatures, they have gained little commercial attention due to the high cost of raw materials and many processing steps. The traditional MgAl_2O_4 spinel manufacturing process involves calcining a combination of metal oxides at high temperatures (1625°C for 2 hours), which has the disadvantages of large aggregates and inhomogeneous compositions.

According to recent studies, combustion synthesis for the creation of binary oxides has a number of advantages, including homogeneity, high purity, the formation of crystallite oxide powders in shorter time periods, and the use of less external energy [53-54]. Magnesium aluminate spinel has long been recognised as an essential ceramic material since it is the only stable compound in the MgO-Al₂O₃ system. Its characteristics, uses, and various processing methods have all been documented in numerous studies [55]. A variety of methods have been used extensively, including conventional solid-state reaction (SSR), sol-gel, spray drying (atomization), and organic gel-assisted citrate complexation [56].

However, several of these synthesis processes are complex and expensive, making large-scale manufacture challenging. Furthermore, conventional synthesis methods employ high-temperature solid-state processes, which lead to porosity destruction and low BET surface areas, limiting the catalytic effectiveness of the resulting spinel materials. As a result, developing an effective method for the controlled synthesis of a porous spinel with a high BET surface area is very desirable. The use of a hard or soft template in the preparation process is usually popular because it results in the production of porosity and a large surface area [57-63]. However, templating methods are difficult, time-consuming, and expensive, limiting scalable manufacturing for commercialization. Sol-gel has various benefits over the other methods for making magnesium aluminate spinel, including excellent purity, chemical homogeneity, and low calcination temperatures [64- 66]. Metal alkoxides, on the other hand, are frequently utilised in this approach. The cost of these metal alkoxides is often expensive, making them unsuitable for commercial scale synthesis. Furthermore, some of them are light, moisture, and heat activated, making them unsuitable for industrial use. To solve the aforementioned issues, various attempts have been made to develop a sol-gel technique based on non-alkoxide based precursors. To overcome this issue, epoxide 93 was used as a gelation agent in this case [67,68]. When compared to other traditional ways, it necessitates a less complicated procedure with various benefits, including low cost and low temperature requirements.

2.3. Various Route of Synthesis of MgAl₂O₄ Spinel:

2.3.1. Vahid et al.[70] successfully synthesized MgAl₂O₄ nanoparticles. The combustion method was used by them to make MgAl₂O₄ nanoparticles. Without additional purification, magnesium nitrate hexahydrate (Mg(NO₃)₂·6H₂O), aluminium nitrate nonahydrate (Al(NO₃)₃·9H₂O), and urea (NH₂CONH₂) were used.

2.3.2. According to Gilvan et al.[71] MgAl₂O₄ nanoparticles were synthesised by mixing Aluminum Nitrate and Magnesium Nitrate as precursors and Gelatin as an organic precursor. The effect of calcination temperature and duration on the structural and morphological characteristics of the resultant materials was investigated. Aluminum Nitrate and Magnesium Nitrate were employed in a 2:1 ratio as a metal precursor. The size of the crystals ranged from 12.4 to 55.5 nm.

2.3.3. Viacheslav et al.[72] prepared MgAl₂O₄ nanoparticles from raw amorphous magnesite and γ -Al₂O₃ nano powders as starting materials for periclase-magnesium aluminate spinel ceramics. Magnesite was annealed at 800°C for two hours. The hydrothermal process was used to create a nano sized γ -Al₂O₃ powder. The Nano powders were then combined and milled in a ball mill for 30 minutes. Periclase-magnesium aluminate spinel ceramic specimens were compacted by bi-directional axial compression and sintered at 1500°C for 2 hours at the maximum temperature. The ceramics' microstructure and mechanical characteristics were evaluated. The researchers created dense periclase-magnesium aluminate spinel ceramics with a density of 3.3 g/cm³ and a compressive strength of more than 300 MPa.

2.3.4. Abdi et Al [69] successfully synthesized MgAl₂O₄ nanoparticles by solid state exchange reaction. Aluminium chloride and magnesium chloride with sodium hydroxide and tiny amount of water were used by them. Precursors were combined and put to high energy ball milling for a brief time yielded MgAl₂O₄ nanoparticles. The milled powder was then heated for 2 hours at 400°C to 1200°C. After characterisation a nano phased pure with an average particle size of 8-12 nm was produced. Then it was sintered at 1500°C resulting in a theoretical density of 93.8 percent.

2.3.5. Li et al.[73] shows Anhydrous aluminium chloride (AlCl_3) and anhydrous magnesium chloride (MgCl_2) were used as aluminium and magnesium precursors, respectively, in the synthesis of MgAl_2O_4 spinel. As an oxygen donor, anhydrous ethanol ($\text{C}_2\text{H}_5\text{OH}$) was used, and dichloromethane (CH_2Cl_2) was used as a solvent. Analytically pure source materials were used without further purification. After characterisation, it was observed that the MgAl_2O_4 spinel had a mesoporous structure with pore diameters ranging from 3 to 50 nm, as well as better sintering capabilities.

2.3.6. Ganesh et al.[74] shows in their experiment that different types of dense stoichiometric and nonstoichiometric magnesium aluminate (MgAl_2O_4) spinel ceramics were prepared using different commercially available alumina such as Aluminum trioxide and aluminium oxide and magnesia raw materials such as Magnesium hydroxide and caustic MgO prepared from sea water magnesia using a conventional double-stage firing process. All of the calcined powder was processed in a rotary mill until the average particle size was obtained during spinel preparation. Following that, Stoichiometric, magnesia-rich, and alumina-rich spinels were sintered for 1-2.5 hours at $1500^\circ\text{-}1800^\circ\text{C}$. Measurements of bulk density, apparent porosity, and water absorption capacity, as well as microstructural observations, were used to examine the impact of different processing parameters on the densification behaviour of MAS. The majority of the MAS compositions tested had outstanding sintering properties.

2.3.7. Padmaraj et al.[75] showed in their experiment that nanocrystallite spinel type magnesium aluminate (MgAl_2O_4) ceramic material was synthesized using the sol gel combustion process. The synthesis was carried out using Magnesium Nitrate ($\text{Mg}(\text{NO}_3)_2 \cdot 6\text{H}_2\text{O}$), Aluminium Nitrate ($\text{Al}(\text{NO}_3)_3 \cdot 9\text{H}_2\text{O}$), and glycine ($\text{NH}_2 \cdot \text{CH}_2 \cdot \text{COOH}$) for the preparation of nanocrystallite MgAl_2O_4 spherical particles using the glycine assisted gel combustion method, in which Magnesium and Aluminium (1:2), as well as the fuel glycine, were dissolved separately with the required quantity of distilled water. The adsorption method was used to determine the specific surface area of the prepared nanocrystallite MgAl_2O_4 powder, which was found to be $162.704 \text{ m}^2/\text{gm}$. At 573K, the predicted conductivity of a nanocrystallite MgAl_2O_4 pellet is $4.92131013 \text{ S cm}^{-1}$. The activation energy of a magnesium aluminate solution was analyzed to be $E_1 = 0.1828 \text{ eV}$ (503 K) and $E_2 = 0.8791 \text{ eV}$ (>503 K) in two different temperature dependent conductivity areas. From the studied impedance data, the conductivity, dielectric constant, and dielectric loss of the nanocrystallite

MgAl₂O₄ sample were determined, and the observed results were analysed and explained using known theoretical models.

2.4. Selection Of Citric Acid as the fuel agent:

2.4.1. Golyeva et al.[76] used a modified Pechini method to produce nanocrystallite aluminium magnesite spinel powders doped with europium ions in their work. As a result, crystallite hydrates of Eu₂O₃, Al(NO₃)₃·9H₂O, and Mg(NO₃)₂·6H₂O were chosen as starting reagents. To make the nitrate solution Eu(NO₃)₃, Eu₂O₃ was dissolved in concentrated nitric acid, while Al(NO₃)₃·9H₂O and Mg(NO₃)₂·6H₂O were dissolved in distilled water. After mixing and heating both solutions, citric acid was added (at a volume ratio of 1:1) to the resulting combination, resulting in the creation of citric metal complexes [Me(C₆H₈O₇)₃](NO₃)₃. The mixture was heated to eliminate surplus water after adding ethylene glycol to citric acid solution in a 1:4 ratio. The poly esterification method resulted in a polymeric gel. The gel was then calcined at temperatures of 500, 600, and 700°C with a 1.5-hour soaking time. The resulting powder was then combined in a weight ratio of 1:1 with potassium chloride and calcined for a second time at a higher temperature (800, 850, 900, 950, 1000, 1100, 1200 °C) for a period of time (1, 2, 3, 4 h). The powder was centrifuged after the second calcination stage, washed three times with distilled water to remove potassium chloride, and then dried. As a result, MgAl₂O₄: Eu³⁺ nanocrystallite powders with different temperatures and durations of calcination stages were synthesized.

2.4.2. Miroliaee et al[77] demonstrated the synthesis of MgAl₂O₄ via thermal breakdown of [Mg(H₂O)₆] [Al(dipic)]₂·6H₂O as an ion-pair complex precursor by using an ion pair complex precursor technique to fabricate high surface area nano powder of MgAl₂O₄ spinel. Two more samples were made using the co-precipitation and citrate sol-gel techniques for comparison. The ion-pair complex precursor approach has the shortest crystallite size (8.7 nm) and thus the largest BET surface area (203.4 m²/g) of the three ways to create MgAl₂O₄ spinel, suggesting fabrication method influence.

2.4.3. Sanjabi et al.[78] demonstrated that nanocrystallite MgAl_2O_4 spinel were successfully synthesised using Aluminium Nitrate ($\text{Al}(\text{NO}_3)_3 \cdot 9\text{H}_2\text{O}$) and Magnesium Nitrate ($\text{Mg}(\text{NO}_3)_2 \cdot 6\text{H}_2\text{O}$) by modified sol gel process. Anhydrous citric acid was gently added to this solution after Magnesium Nitrate was initially dissolved in diethyl glycol monoethyl ether, and then sintered. FESEM analysis was done after synthesization and calcination. The spherical nanoparticle they get is in the 12 nanometer range.

2.4.4. Rahmat et al[79] performed single stage solid state fusion of Magnesium aluminate (MgAl_2O_4) with citric acid as a fuel agent in their experiment.

The samples were made under various annealing circumstances, including as temperature and duration. Using a mortar and pestle, the stoichiometric ratios of $\text{Mg}(\text{NO}_3)_2 \cdot 6\text{H}_2\text{O}$, $\text{Al}(\text{NO}_3)_3 \cdot 9\text{H}_2\text{O}$, and $\text{C}_6\text{H}_8\text{O}_7 \cdot \text{H}_2\text{O}$ in 1:2:3 were mixed and rigorously pulverised for at least 1 hour.

After that, the crushed mixture was placed in a crucible and baked for 2 hours in an oven at 100°C . The size of the crystallites increased as the calcination temperature increased, but the MgAl_2O_4 spinel's specific surface area shrank. Its catalytic activity in the steam reforming of methane has indicated that the MgAl_2O_4 spinel, which has a large surface area, tiny crystallite size, and low aggregations, can result in a high conversion of methane (57 percent) in the first 180 minutes of reaction. Meanwhile, due to thermal sintering at high temperatures, the sample annealed at 1000°C had poor catalytic activity.

2.5. Microhardness of MgAl₂O₄ spinel[80]:-

Prasad Ram Chavan et al checked microhardness of MgAl₂O₄ using electronic micro hardness testing machine. They made MgAl₂O₄ samples with varied Mg and Al ratios. They found that the sample M75Al25 has a lower microhardness rating. They also found that as the weight percent of magnesium nitrate increases, the microhardness decreases.

CHAPTER 3

EXPERIMENTAL WORK

3.1. PREAMBLE:

The Magnesium Alumina spinel powder was synthesised using the sol gel synthesis procedure in this experiment. Magnesium Nitrate Hexahydrate ($\text{Mg}(\text{NO}_3)_2 \cdot 6\text{H}_2\text{O}$) and Aluminium Nitrate Nonahydrate ($\text{Al}(\text{NO}_3)_3 \cdot 9\text{H}_2\text{O}$) as precursors were mixed with 5-7 ml DI water and Citric Acid Anhydrous ($\text{C}_6\text{H}_8\text{O}_7$) as the fuel agent to synthesize MgAl_2O_4 . By increasing Citric Acid Anhydrous in 1:2:1.25, 1:2:1.5, and 1:2:1.75 ratios, $\text{Mg}(\text{NO}_3)_2 \cdot 6\text{H}_2\text{O}$ and $\text{Al}(\text{NO}_3)_3 \cdot 9\text{H}_2\text{O}$ and $\text{C}_6\text{H}_8\text{O}_7$ were mixed in the ratio. As a result, three distinct ratio samples of MgAl_2O_4 spinel were produced. Not only varying Citric Acid Anhydrous but it will also be attempted to manage lowering the temperature and lowering the heat treatment time of obtaining spinel.

3.2. SAMPLE PREPARATION:

3.2.1. Preparation Of Solution:

The MgAl_2O_4 had been prepared by the sol gel route.

Raw Materials used were

Magnesium Nitrate Hexahydrate ($\text{Mg}(\text{NO}_3)_2 \cdot 6\text{H}_2\text{O}$) and Aluminium Nitrate Nonahydrate ($\text{Al}(\text{NO}_3)_3 \cdot 9\text{H}_2\text{O}$) as the precursor and Citric Acid Anhydrous ($\text{C}_6\text{H}_8\text{O}_7$) as fuel agent

These raw materials were taken varying Citric Acid Anhydrous in the 3 different ratio of molar weight in 1:2:1.25, 1:2:1.5 and 1:2:1.75 and were mixed together (FIG 3.1) along with 10 ml DI water.

3.2.2. Heating and Drying Of Solution:

After combining them together in the aforesaid molar ratio, they were heated at 80°C for 3 to 4 hours (FIG 3.3) in each of the given ratio samples to form the gel in the sol gel method. Because of the gel formation that developed quickly due to the fuel used, only a tiny amount of distilled water was being supplied. 10 ml. water were used (FIG 3.2). The solution undergoes a rapid rise in viscosity during gel formation, which corresponds to the shift from a viscous fluid to an elastic gel. So, in that gel formation, when the gas was unable to evaporate, the gel turned into little yellowish colour. It was then heated in an Ultra sonicator for 5-8 hours (FIG 3.4) at a temperature of 50°C , which helped the formation of synthesis more homogeneous, which was exactly needed. Though the time required is substantially longer, the vibrating of the molecules was allowed for easy separation and helped in the evaporation of the vapour.



FIG-3.1-RAW MATERIALS WERE BEING WEIGHTED ACCORDING TO MOLAR RATIOS



FIG-3.2-AFTER WEIGHING,RAW MATERIALS WERE MIXED TOGETHER WITH 10ml. DISTILLED WATER



FIG-3.3- AFTER COMBINING TOGETHER, THEY WERE HEATED AT 80°C FOR 3 TO 4 HOURS TO FORM GEL



FIG-3.4-DRIED GEL WAS HEATED IN ULTRASONICATOR

3.3. Calcination:

After the pore liquid had been removed, heat treatment was required to transform the material into a catalytically usable form. To burn out any leftover organics, the heating was done in the presence of a reactive gas (here, moving air).

The sample was placed in a ceramic boat and placed in the furnace for calcination(FIG-3.5).

- First, temperature must be determined, at which calcination would take place, which will remain constant during the process. Temperatures of 650, 700, and 800⁰ Celsius were used.
- After that, the holding period was determined, which was between 4,5 and 6 hours for each sample with the same molecular ratio. Because an electric furnace was used, the programme was being set first.
- Then the cooling was done which is not in controlled programme. So certain time is needed to cooling the furnace.



FIG-3.5.-GEL IS PLACED IN A BOAT AND PLACED IN A FURNACE FOR CALCINATION

3.4. Hand Grinding Of Calcined Powder:

The calcined powder were grounded using an Agate Mortar pestles after being calcined at various temperatures to better their characterization.



FIG-3.6-CALCINED POWDER IS GROUND IN AGATE MORTAR

3.5. PRESSING AND COMPACTING FOR MICROHARDNESS TEST:

After calcination, the powder was mixed with PVA (Polyvinyl Alcohol) for material binding, which was done at a ratio of 2 wt% percent PVA and with that 98:1 water and PVA. The water and PVA were heated to 50°C until they dissolved, and then dissolved water with PVA were poured with the powder $MgAl_2O_4$. Then the mixture was heated and sonicated until $MgAl_2O_4$ dissolved entirely. The powder combination was then placed into a 50 mm diameter mould cavity in a die system and pressed using 200 MPa uniaxial pressure in hydraulic cold press (FIG-3.7). Then cylindrical spinel pellets with various material ratios were created.



FIG-3.7-PVA MIXED CALCINED POWDER IS BEING PRESSED IN HYDRAULIC COLD PRESS

3.6. CURING:

For around 1 hour, the compacted sample was cured at 400⁰C to remove the PVA. Then the pellets were well sintered at 1400⁰C with holding time for 2 hours. This was done for

- Elimination of residual water, volatile matters if presence in the sample.
- Development of sufficient strength and proper binding of the constituents so that pellets could be used for micro hardness test.



FIG-3.8-AFTER SINTERING DEVELOPED PELLETS

3.7. Surface Finishing:-

Surface finishing of the sintered pellets were done with the help of diamond paste and a glass. Pellets were being rubbed continuously till the plane surface could be got. After surface finish Pellets were undergone for microhardness testing.

3.7. CHARACTERIZATION:

3.7.1. DTA/TGA Analysis:

Differential Thermal Analysis is abbreviated as DTA, and Thermo-Gravimetric Analysis is abbreviated as TGA. A sample in one crucible and a reference in another are heated simultaneously in the DTA analysis. The temperature difference between the sample and the reference is measured in DTA analysis. We can simply establish whether the process is exothermic or endothermic based on this information.

TGA is a technique that precisely detects mass and changes in mass as temperature rises. The Diamond DT-TGA can also analyse DSC using appropriate software to map heat flow vs. temperature. This method can monitor both weight change and heat flow at the same time, allowing every phase shift to be precisely identified, as most phase changes occur without a change in weight. The schematic view and image of the DT-TGA instrument are shown below (FIG-3.9)–



FIG-3.9-DTA-TGA MACHINE

Nitrogen Atmosphere (150ml/min) Platinum crucible used with alpha alumina powder as reference.

3.7.2 XRD Analysis:

After the material has been synthesised, it must be characterised in order to determine its phase. The XRD analysis is an analytical technique used to obtain more detailed information about crystallite compounds, such as crystallite phase identification and quantification. When we need to identify a contaminant for additive identification of foreign phases for purity analysis of crystallite powders, this is a valuable technique.

X-rays are waves of electromagnetic energy, and crystals are regular arrays of atoms. Scattering of incident X-rays occurs due to the interaction of incident X-rays and the electrons of crystal atoms. Elastic scattering is the name for this phenomena, and the electron is the scatterer. The scatterers in a regular array produce a regular array of spherical waves. These waves cancel each other out in most directions due to destructive interference, but they add constructively in a few select directions, as indicated by Bragg's law:

$$n\lambda=2d\sin\theta$$

Where d denotes the distance between diffracting planes, θ is the incident angle, n is an integer, and λ is the beam wavelength.

Reflections on the diffraction pattern reveal the precise directions. X-ray diffraction patterns emerge from electromagnetic waves striking a regular array of scatterers.

X-rays are used to produce the diffraction pattern because their wavelength, λ , is often the same order of magnitude as the spacing, d , between the crystal planes (1-100 angstroms)

The information which we get from diffraction patterns are

- Crystal Quality
- Texture to some extent
- Crystal Size
- Crystal Structure.
- Phase Identification

A graph in the form of intensity v/s 2 theta is being drawn using the XRD analysis data. Peaks in the graph would represent the crystallisation of a specific phase. The information from each peak (angle, intensity, flex width, and d-value) must be compared to JCPDS data. Joint Committee on Powder Diffraction Standards is an acronym for JCPDS. This is a database of standard XRD reference patterns.



Figure 3.10: X-Ray Diffraction Machine

For the synthesized sample X-Ray Diffraction analysis was carried out with Bruker D8 Advance of all the samples under identical conditions with Cu K α radiation whose-

Tube voltage is 40 kV

Tube current is 40 mA.

Scan Range: 10 $^{\circ}$ -90 $^{\circ}$

Scan Mode: Continuous

Speed: 1 $^{\circ}$ /min

3.7.3. FTIR Analysis:

The preferred method of infrared spectroscopy is known as Fourier transform infrared (FTIR). When infrared radiation travels through a sample, some of it is absorbed by the sample and the rest passes through (is transmitted).

The resulting signal at the detector is a spectrum that represents the sample's molecular "fingerprint." Because different chemical structures (molecules) give different spectral fingerprints, infrared spectroscopy is useful.

So, FTIR analysis is done for following reasons,

1. The Fourier Transform converts the detector output into a spectrum that can be interpreted.
2. The FTIR produces spectra that contain patterns that provide structural information.

We can get to know from the FTIR analysis that

- If In the sample, there is an unknown element.
- Determine the sample's quality or consistency.
- Calculate the total amount of each element in the combination.

The size of the peaks in the spectrum shows the amount of material present, while their location reveals typical bonds. The sample was prepared for FTIR spectroscopy by adding KBr to the sample and compressing it with hydraulic pressure to form a pellet. For the reference material, one KBr pellet was also manufactured as reference material.

We can determine if the vibration is bending or stretching from the FTIR analysis by plotting data to the signal and wavelength graph. Because bending is easier than stretching, bending vibrations are lower in energy than stretching vibrations for the same bond.



Figure 3.11: SHIMADZU IR PRESTIGE-21 FTIR SPECTROMETER

3.7.4. FESEM Analysis:

In the field emission scanning electron microscope (FESEM), a sample surface has been imaged by raster scanning over it with a high-energy beam of electrons. Electrons interact with the atoms in the sample to produce signals that carry information about the sample's surface topography, composition, and other characteristics like electrical conductivity.

The electron gun's job is to deliver a large, stable current in a tiny beam.

The image quality will be significantly improved because the FE source is around 1000 times smaller than that in a typical microscope with a thermal electron gun; for example, resolution will be on the order of 2 nm at 1 keV and 1 nm at 15 keV.

In Nanoscience, the size range is often hundreds of nanometers down to the atomic level (about 0.2 nm), where materials (nano materials) might have different or better chemical/physical properties when compared to similar materials at a bulk size. [41-43].



Figure 3.12: FESEM Machine ZEISS

3.8. Microhardness Testing:-

A diamond indenter is used to make an indentation on the specimen during microhardness testing by applying a load P . With the use of a calibrated optical microscope, the size d of the resulting indentation is measured, and the hardness is determined by the mean stress applied beneath the indenter.(FIG-3.12)

The following are the equations for Vickers hardness (H_V) and Knoop hardness (H_K):

$$H_K = 14228(P/d^2) \text{ kgf mm}^2$$

$$H_V = 1854.4(P/d^2) \text{ kgf mm}^2$$

The dimensions of stress, load P , and diagonal length d are measured in gram force and micrometre, respectively, In these equations (Figure 3.12). The first equation is based on the impression surface area; the second is based on the projected area of the impression and the length of the long diagonal.

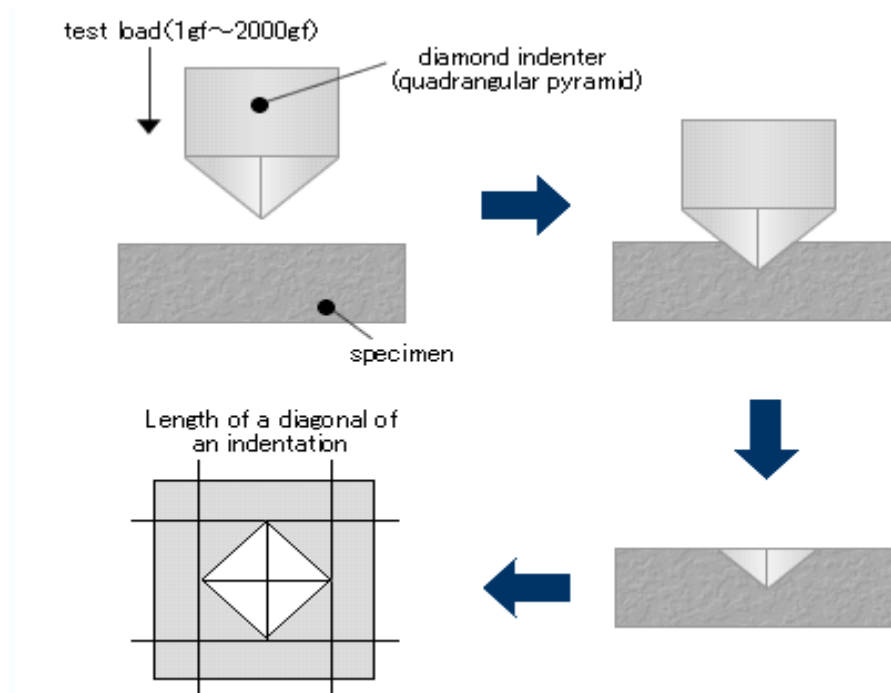


FIG-3.12-SCHEMATIC DIAGRAM OF MICRO-HARDNESS TESTING



FIG-3.13-Pellet Is Being Placed Under Indenter And Micro-Hardness Is Being Tested

CHAPTER 4

RESULT AND DISCUSSION

4.1. DTA/TGA Analysis :

Thermal analysis of the obtained gel of Mg:Al:CA=1:2:1.5 within the temperature range 0°C-1000°C at the rate of 10°C/min is used for DTA-TGA analysis. The graph is shown in Figure 4.1.

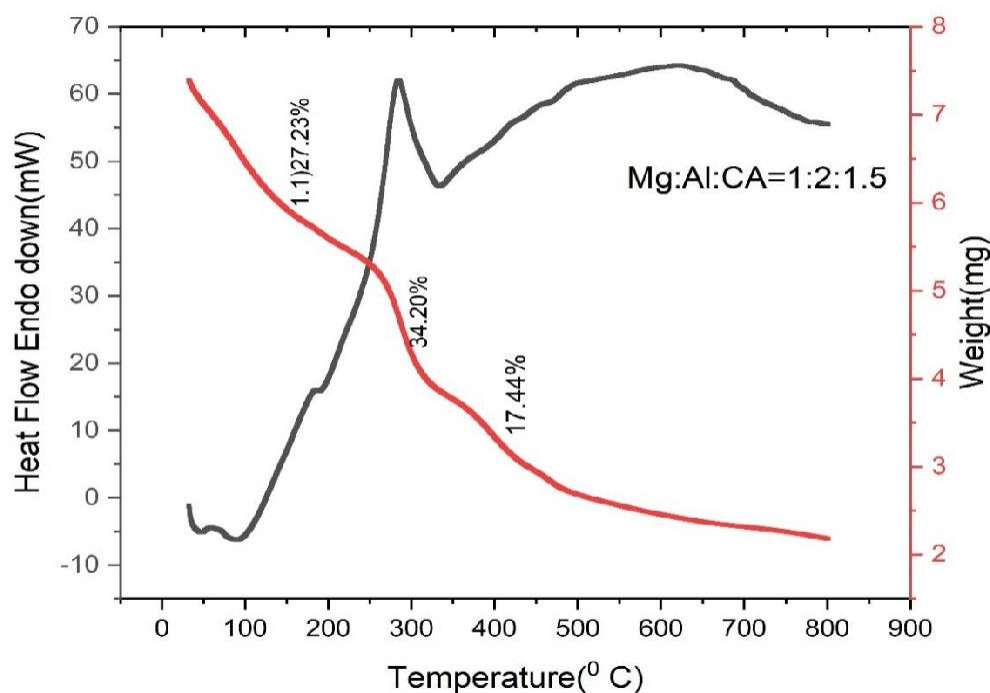


FIG-4.1-DSC-TGA analysis of mixture of Mg:Al:CA=1:2:1.5 within the temperature range 0°C-1000°C at the rate of 10°C/min

We can deduce the following from the TGA graph,

1.1) Examining the graph we come to know at 33.04°C-240.10°C weight decrease. Water molecules are most likely to be responsible for 27.23% of the weight reduction.

1.2) Examining the graph at we also understand at 240.10°C -311.93°C weight loss occurs. This 34.20 percent weight loss is most likely due to the OH molecules. [34]

1.3) At 311.93°C -398.01°C, the weight loss is roughly 12.498 percent, which corresponds to the removal of amino acids and reaction agent citric acid compounds.

1.4) A higher temperature is required to break the bonds between citric acid and spinel.

1.5) It can be seen from the graph, weight loss remains steady above 600⁰ C, indicating the formation of crystallite structure.

According to the DTA plot ,

- 1.The endothermic reaction happened at 89.07⁰ C.
- 2.At 283.86⁰ C, a strong exothermic reaction occurs, resulting in the release of chemically contained moisture.
- 3.At 599.84⁰C, the tiny exothermic reaction occurs, which corresponds to the reaction agent citric acid and nitrate breakdown

4.2. XRD Study of Magnesium Aluminate Spinel:

XRD or x-ray diffraction are basically being done to analyse the structure of crystallite materials. Here MgAl_2O_4 spinels are produced calcination of dried gel precursors at different temperature and with different calcination times. For the XRD analysis Citric Acid has been used as fuel agent and the composition were varied which corresponds to Mg:Al:CA are in the ratio of 1:2:1.25, 1:2:1.5, 1:2:1.75, 1:2:1.5. Those samples are calcined at different temperature from 650, 700, 800^o C with different calcination time as 4, 5, 6 hours. These samples are undergone XRD analysis and resulting peaks have been identified with the comparison of standard JCPDS library.

Here the calcined powder are being characterized by Bruker D8 Advance, using $\text{Cu K}\alpha$ radiation.

4.2.1. XRD Analysis of MgAl_2O_4 in Citric acid molar ratio 1.25:

$\text{Mg}(\text{NO}_3)_2 \cdot 6\text{H}_2\text{O}$ and $\text{Al}(\text{NO}_3)_3 \cdot 9\text{H}_2\text{O}$ were mixed with Citric Acid as fuel agent in the ratio of 1:2.75:1.25 and sol gel route were used. After gel formation calcination was done at different temperature ranging from 650^o, 700^o, 800^o C and with different calcination time as 4, 5, 6 hours. White powder samples were prepared which were undergone XRD analysis and resulting peaks have been identified with the comparison of JCPDS library.

XRD of Spinel(Citric acid in 1.25 molar ratio) at 650^oC(6 hours):

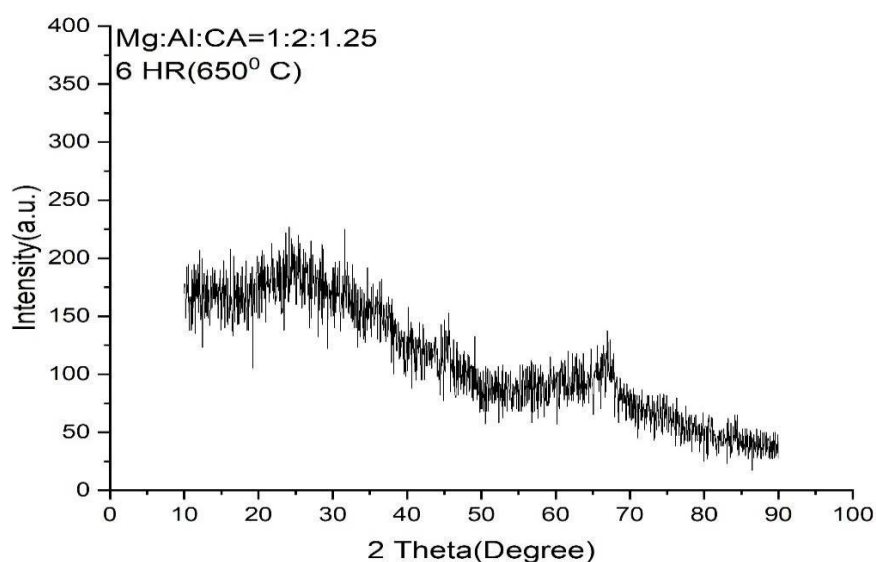


FIG-4.1- XRD GRAPH OF SPINEL(CITRIC ACID IN 1.25 MOLAR RATIO) AT 650^oC(6 HOURS)

From the XRD graph(FIG-4.1) 1 small peak can be got. Due to much vibration proper peak can't be found. From this graph we can understand at 650⁰ C crystallization has been started. The obtained planes comparing to these peaks have been indexed with the assistance of the standard JCPDS library. The Scherrer formula has been used to calculate the material's crystal size. Scherrer formula is

$$d = k\lambda / \beta \cos \theta$$

Where d represents the crystallite size in nm, k = 0.9 is a correction factor, β = full width at half maximum(radian), λ is the wavelength of X-ray source= 0.15406 nm and θ is the Bragg's angle(radians).

| Peak No | d-value of corresponding peak | 2 θ value of corresponding peak | Standard d-value | Planes | Chemical formula of compound | Crystalline size |
|---------|-------------------------------|--|------------------|--------|----------------------------------|------------------|
| 1 | 1.4358 | 66.40 | 1.4289 | (440) | MgAl ₂ O ₄ | 7.578 |

The only crystallite size of the material obtained is 7.578 nm.

XRD of Spinel(Citric acid in 1.25 molar ratio) at 800°C(6 hours):

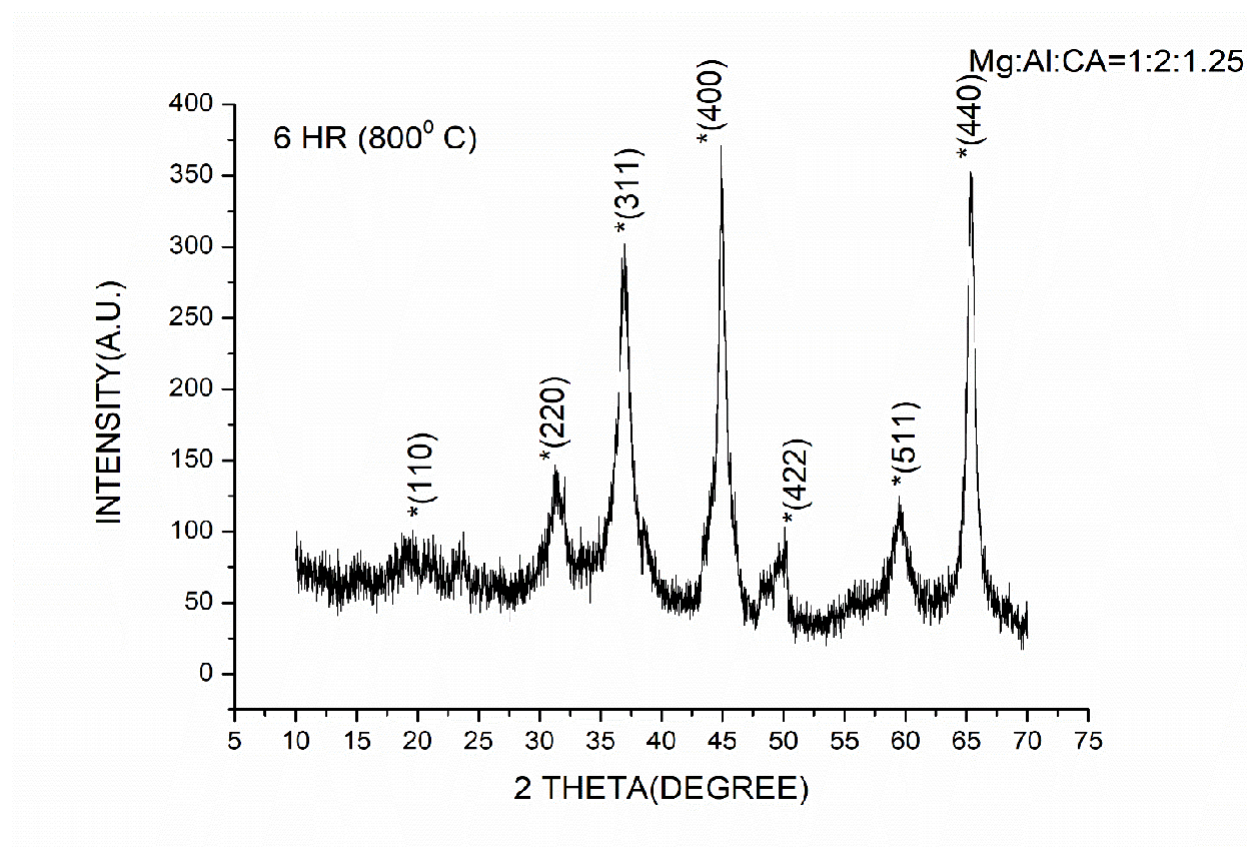


FIG-4.2- XRD GRAPH OF SPINEL(CITRIC ACID IN 1.25 MOLAR RATIO) AT 800°C(6 HOURS)

From the XRD graph(FIG-4.2) 7 peaks can be found. The obtained planes comparing to these peaks have been indexed with the assistance of the standard JCPDS library. There are 7 peaks and each peak proposes the stage which has been crystallized at 800°C is in pure phase of spinel (MgAl_2O_4).

From the XRD graph obtained 2 theta values of the peaks have been used for calculating d-value of the corresponding peak. These d-values have been compared with standard d values of JCPDS library. And these 7 planes resemble the planes of MgAl_2O_4 spinel. These information is used to understand that at 800°C pure phase of spinel is crystallized.

The material's crystallite size remains consistent, ranging from **5.4536 to 10.2692 nm**. Here also Scherrer formula has been used to calculate the material's crystallite size.

Scherrer formula is,

$$d = k\lambda / \beta \cos \theta$$

Where d represents the crystallite size in nm, k = 0.9 is a correction factor, β = full width at half maximum (radian), λ is the wavelength of X-ray source = 0.15406 nm and θ is the Bragg's angle (radians).

| Peak No | d-value of corresponding peak | 2 θ value of corresponding peak | Standard d-value | Planes | Chemical formula of compound | Crystalline size |
|---------|-------------------------------|--|------------------|--------|----------------------------------|------------------|
| 1 | 4.6670 | 18.90 | 4.6653 | (111) | MgAl ₂ O ₄ | 5.8675 |
| 2 | 2.8404 | 31.46 | 2.8569 | (220) | MgAl ₂ O ₄ | 5.4536 |
| 3 | 2.4321 | 36.92 | 2.4363 | (311) | MgAl ₂ O ₄ | 5.5802 |
| 4 | 2.0146 | 44.95 | 2.0201 | (400) | MgAl ₂ O ₄ | 8.0479 |
| 5 | 1.6434 | 55.63 | 1.6494 | (422) | MgAl ₂ O ₄ | 7.6989 |
| 6 | 1.5416 | 59.53 | 1.5551 | (511) | MgAl ₂ O ₄ | 5.667 |
| 7 | 1.4263 | 65.37 | 1.4284 | (440) | MgAl ₂ O ₄ | 10.2692 |

4.2.2. XRD Analysis of MgAl₂O₄ in Citric acid molar ratio 1.5:

Mg(NO₃)₂.6H₂O and Al(NO₃)₃.9H₂O were mixed with Citric Acid as fuel agent in the ratio of 1:2:1.5 and sol gel route route were used. After gel formation calcination was done at different temperature ranging from 650^o, 700^o, 800^o C and with different calcination time. White powder samples were prepared some of those were undergone XRD analysis and resulting peaks have been identified with the comparison of JCPDS library.

XRD of Spinel(Citric acid in 1.5 molar ratio) at 800°C(6 hours):

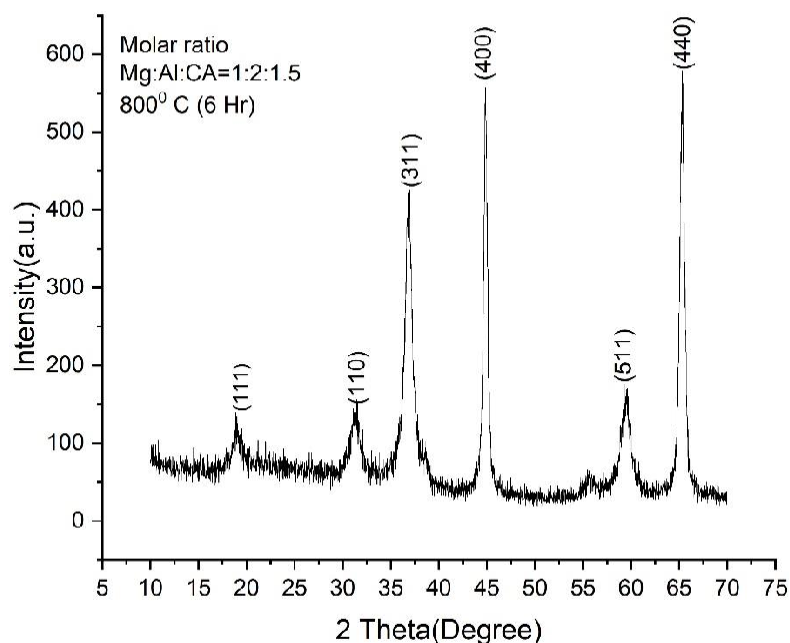


FIG-4.3- XRD GRAPH OF SPINEL(CITRIC ACID IN 1.5 MOLAR RATIO) AT 800°C(6 HOURS)

From the XRD graph(FIG-4.3) 6 peaks can be found. The obtained planes comparing to these peaks have been indexed with the assistance of the standard JCPDS library. From 6 peaks 5 peaks propose the stage which has been crystallized at 800°C is in pure phase of spinel $MgAl_2O_4$, and remaining 1 peak resembles Al_2O_3 according to JCPDS library.

From the XRD graph obtained 2 theta values of the peaks have been used for calculating d-value of the corresponding peak. These d-values have been compared with standard d values of JCPDS library. And these 6 planes resemble planes of $MgAl_2O_4$ spinel and remaining one resembles the plane of Al_2O_3 . These information is used to understand that at 800°C and 6 Hr calcination 85.71% pure phase of spinel is crystallized.

The material's crystallite size remains consistent, ranging from **6.9429 nm to 16.3134 nm**. Here also Scherrer formula has been used to calculate the material's crystallite size. Scherrer formula is

$$d = k\lambda / \beta \cos \theta$$

Where d represents the crystallite size in nm, k = 0.9 is a correction factor, β = full width at half maximum(radian), λ is the wavelength of X-ray source= 0.15406 nm and θ is the Bragg's angle(radians).

| Peak No | d-value of corresponding peak | 2 θ value of corresponding peak | Standard d-value | Planes | Chemical formula of compound | JCPDS Card No | Crystalline size |
|---------|-------------------------------|--|------------------|--------|----------------------------------|---------------|------------------|
| 1 | 4.547791 | 19.50342 | 4.7192 | (111) | MgAl ₂ O ₄ | 77-0436 | 7.942916 |
| 2 | 2.852211 | 31.337 | 2.8204 | (110) | Al ₂ O ₃ | 86-1410 | 6.942914 |
| 3 | 2.436142 | 36.86615 | 2.4645 | (311) | MgAl ₂ O ₄ | 77-0436 | 8.1529 |
| 4 | 2.018318 | 44.87241 | 2.0201 | (400) | MgAl ₂ O ₄ | 77-0435 | 16.3134 |
| 5 | 1.553346 | 59.45788 | 1.5551 | (511) | MgAl ₂ O ₄ | 77-0435 | 6.904549 |
| 6 | 1.427366 | 65.32173 | 1.4284 | (440) | MgAl ₂ O ₄ | 77-0435 | 14.40975 |

XRD of Spinel(Citric acid in 1. 5 molar ratio) at 800°C(4 hours):

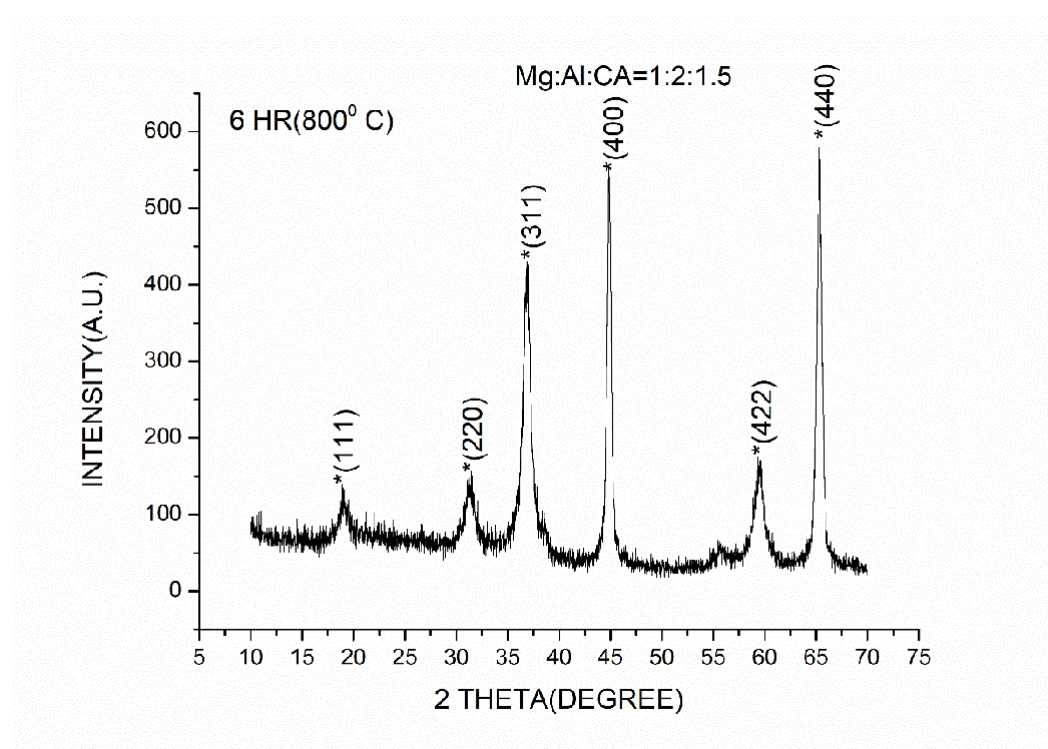


FIG-4.4- XRD GRAPH OF SPINEL(CITRIC ACID IN 1.5 MOLAR RATIO) AT 800°C(4 HOURS)

From the XRD graph (FIG-4.4) 6 peaks can be found. The obtained planes comparing to these peaks have been indexed with the assistance of the standard JCPDS library. From 6 peaks 5 peaks resemble the stage, which has been crystallized at 800°C for 4 hours are in pure phase of spinel MgAl₂O₄, and remaining 1 peak (110) resembles Al₂O₃ according to JCPDS library.

From the XRD graph obtained 2 theta values of the peaks has been used for calculating d-value of the corresponding peak. These d-values have been compared with standard d values of JCPDS library. And these 5 planes resembles planes of MgAl₂O₄ spinel and remaining one resembles the plane of Al₂O₃. These information is used to understand that at 800°C with 4 hour calcination pure phase of spinel has been crystallized.

The material's crystallite size remains consistent, ranging from **7.1929 nm to 17.2151 nm**. Here also Scherrer formula has been used to calculate the material's crystallite size. Scherrer formula is

$$d = k\lambda / \beta \cos \theta$$

Where d represents the crystallite size in nm, k = 0.9 is a correction factor, β = full width at half maximum (radian), λ is the wavelength of X-ray source = 0.15406 nm and θ is the Bragg angle (radians).

| Peak No | d-value of corresponding peak | 2 θ value of corresponding peak | Standard d-value | Planes | Chemical formula of compound | JCPDS Card No | Crystalline size |
|---------|-------------------------------|--|------------------|--------|----------------------------------|---------------|------------------|
| 1 | 4.445316 | 19.9576 | 4.7192 | (111) | MgAl ₂ O ₄ | 77-0436 | 7.237689 |
| 2 | 2.843415 | 31.4364 | 2.8204 | (110) | Al ₂ O ₃ | 86-1410 | 6.553666 |
| 3 | 2.430452 | 36.9555 | 2.4645 | (311) | MgAl ₂ O ₄ | 77-0436 | 7.192939 |
| 4 | 2.014388 | 44.96472 | 2.0201 | (400) | MgAl ₂ O ₄ | 77-0435 | 17.21511 |
| 5 | 1.552091 | 59.5108 | 1.5551 | (511) | MgAl ₂ O ₄ | 77-0435 | 5.890026 |
| 6 | 1.425596 | 65.41297 | 1.4284 | (440) | MgAl ₂ O ₄ | 77-0435 | 15.08877 |

4.2.3. XRD Analysis of MgAl₂O₄ in Citric acid molar ratio 1.75:

Mg(NO₃)₂.6H₂O and Al(NO₃)₂.9H₂O were mixed with Citric Acid as fuel agent in the ratio of 1:2:1.75 and sol gel route route were maintained. After gel formation calcination was done at different temperature ranging from 650^o, 700^o, 800^o C and with different calcination time. White powder samples were prepared some of those were undergone XRD analysis and resulting peaks have been identified with the comparison of JCPDS library.

XRD of Spinel(Citric acid in 1.75 molar ratio) at 800°C(4 hours):

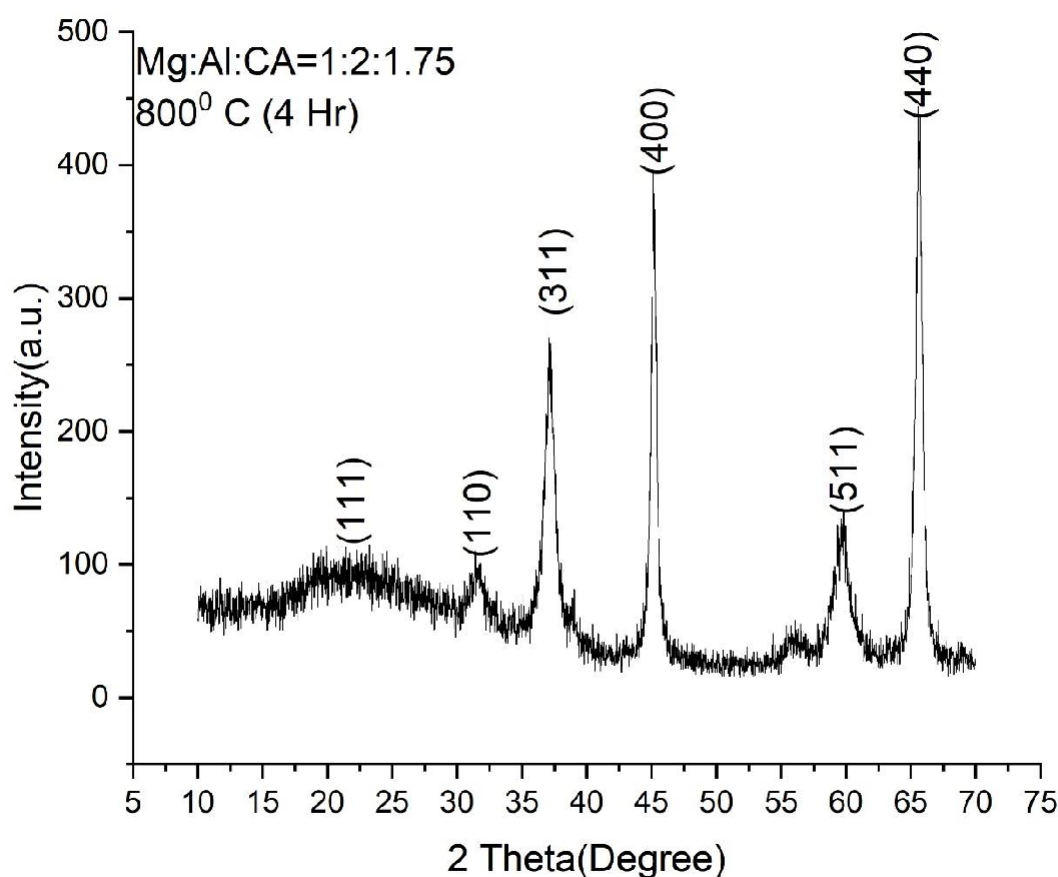


FIG-4.5- XRD GRAPH OF SPINEL(CITRIC ACID IN 1.75 MOLAR RATIO) AT 800°C(4 HOURS)

From the XRD graph(FIG-4.5) 6 peaks can be found. The obtained planes comparing to these peaks have been indexed with the assistance of the standard JCPDS library. From 6 peaks 5 peaks resemble the stage which has been crystallized at 800°C for 4 hours calcination, is in pure phase of spinel $MgAl_2O_4$, and remaining 1 peak(110) resembles Al_2O_3 according to JCPDS library.

From the XRD graph obtained 2 theta values of the peaks have been used for calculating d-value of the corresponding peak. These d-values have been compared with standard d values from JCPDS library. And these 5 planes resemble planes of $MgAl_2O_4$ spinel and remaining one resembles the plane of Al_2O_3 . These information is used to understand that at 800°C with 4 hour calcination 85.71% pure phase of spinel has been crystallized.

The material's crystallite size remains consistent, ranging from **5.8403 nm to 15.16 nm**. Here also Scherrer formula has been used to calculate the material's crystallite size. Scherrer formula is

$$d = k\lambda / \beta \cos \theta$$

Where d represents the crystallite size in nm, $k = 0.9$ is a correction factor, β = full width at half maximum (radian), λ is the wavelength of X-ray source = 0.15406 nm and θ is the Bragg's angle (radians).

| Peak No | d-value of corresponding peak | 2 θ value of corresponding peak | Standard d-value | Planes | Chemical formula of compound | JCPDS Card No | Crystalline size |
|---------|-------------------------------|--|------------------|--------|----------------------------------|---------------|------------------|
| 1 | 4.445316 | 21.81837 | 4.7192 | (111) | MgAl ₂ O ₄ | 77-0436 | 7.360463 |
| 2 | 2.843415 | 31.61073 | 2.8204 | (110) | Al ₂ O ₃ | 86-1410 | 7.769236 |
| 3 | 2.430452 | 37.15094 | 2.4645 | (311) | MgAl ₂ O ₄ | 77-0436 | 7.827343 |
| 4 | 2.014388 | 45.17305 | 2.0201 | (400) | MgAl ₂ O ₄ | 77-0435 | 15.16992 |
| 5 | 1.552091 | 59.67607 | 1.5551 | (511) | MgAl ₂ O ₄ | 77-0435 | 5.840309 |
| 6 | 1.425596 | 65.62967 | 1.4284 | (440) | MgAl ₂ O ₄ | 77-0435 | 13.56897 |

XRD of Spinel(Citric acid in 1.75 molar ratio) at 700°C(6 hours):

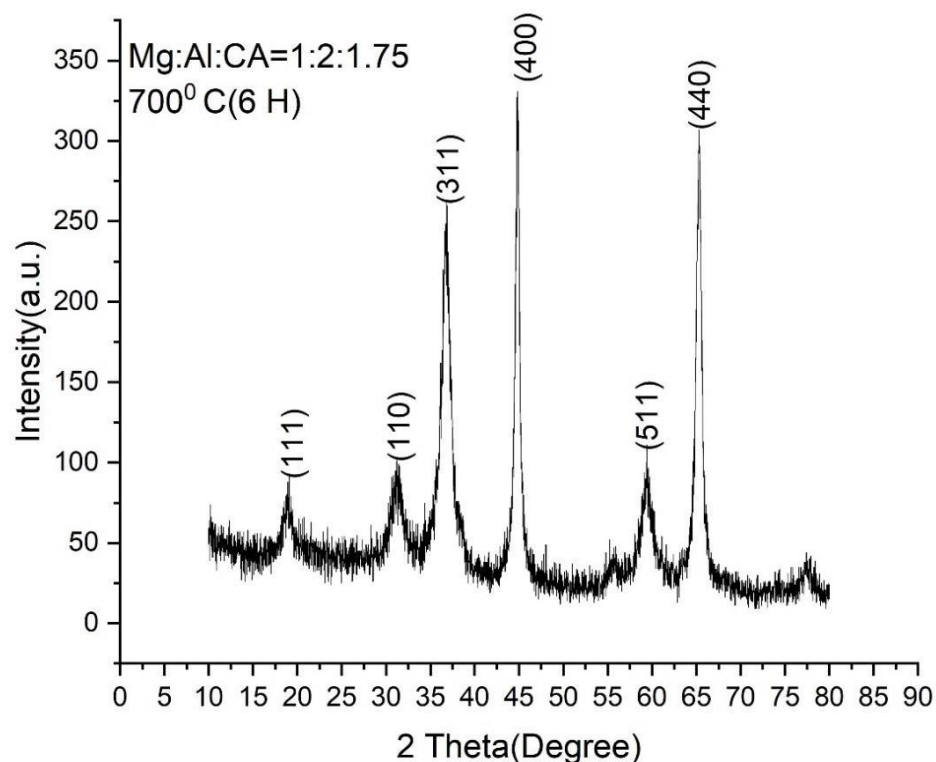


FIG-4.6- XRD GRAPH OF SPINEL(CITRIC ACID IN 1.75 MOLAR RATIO) AT 700°C(6 HOURS)

From the XRD graph(FIG-4.6)6 peaks can be found. The obtained planes comparing to these peaks have been indexed with the assistance of the standard JCPDS library. From 6 peaks 5 peaks propose the stage which has been crystallized at 800°C for 4 hours calcination, resemble the pure phase of spinel $MgAl_2O_4$, and remaining 1 peak(110) resembles Al_2O_3 according to JCPDS library.

From the XRD graph obtained 2 theta values of the peaks has been used for calculating d-value of the corresponding peaks. These d-values have been compared with standard d values from JCPDS library. And these 5 planes resemble planes of $MgAl_2O_4$ spinel and remaining one resembles the plane of Al_2O_3 . These information is used to understand that at 800°C with 6 hour calcination 85.71% pure phase of spinel has been crystallized.

The material's crystallite size remains consistent, ranging from **4.601 nm to 13.19661 nm**. Here also Scherrer formula has been used to calculate the material's crystallite size. Scherrer formula is

$$d = k\lambda / \beta \cos \theta$$

Where d represents the crystallite size in nm, k = 0.9 is a correction factor, β = full width at half maximum(radian), λ is the wavelength of X-ray source= 0.15406 nm and θ is the Braggs angle(radians).

| Peak No | d-value of corresponding peak | 2 θ value of corresponding peak | Standard d-value | Planes | Chemical formula of compound | JCPDS Card No | Crystalline size |
|---------|-------------------------------|--|------------------|--------|------------------------------|---------------|------------------|
| 1 | 4.682488 | 18.93714 | 4.7192 | (111) | $MgAl_2O_4$ | 77-0436 | 6.312717 |
| 2 | 2.855475 | 31.30027 | 2.8204 | (110) | Al_2O_3 | 86-1410 | 4.601001 |
| 3 | 2.441819 | 36.77736 | 2.4645 | (311) | $MgAl_2O_4$ | 77-0436 | 5.775384 |
| 4 | 2.020579 | 44.81945 | 2.0201 | (400) | $MgAl_2O_4$ | 77-0435 | 13.19661 |
| 5 | 1.553915 | 59.43389 | 1.5551 | (511) | $MgAl_2O_4$ | 77-0435 | 5.289686 |
| 6 | 1.427988 | 65.28973 | 1.4284 | (440) | $MgAl_2O_4$ | 77-0435 | 11.2735 |

4.3. FTIR of Spinel(Citric acid in 1.5 molar ratio) at 800°C(6 hours):

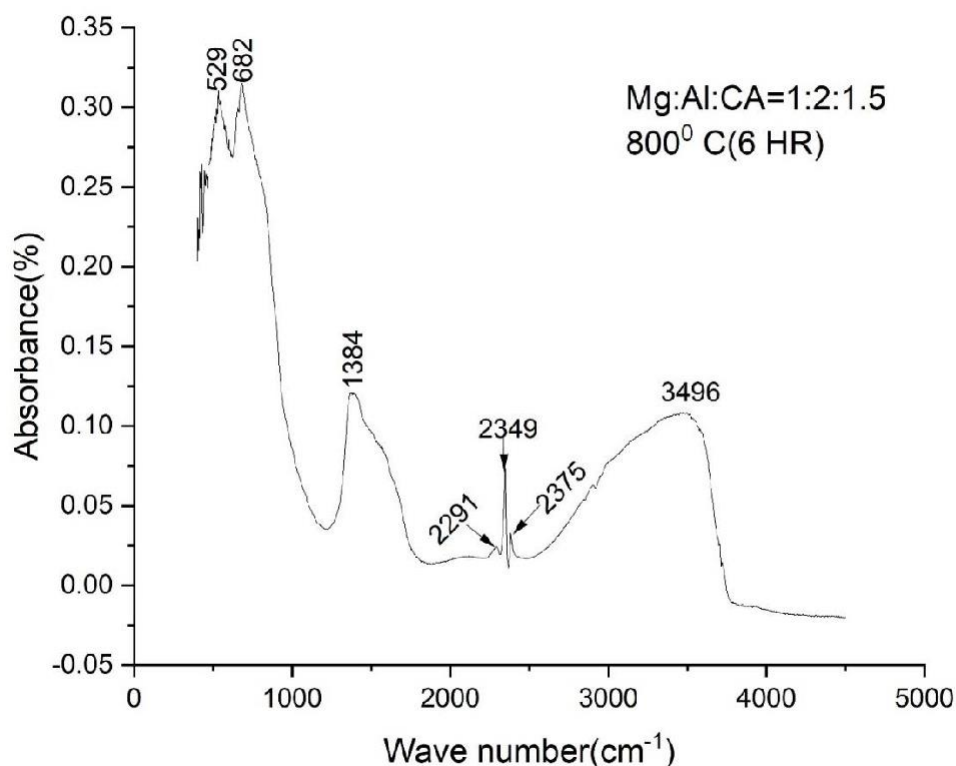


FIG-4.7-FTIR OF SPINEL(CITRIC ACID IN 1.5 MOLAR RATIO) AT 800°C(6 HOURS)

FTIR spectra of calcined samples with Mg, Al, and citric acid molar ratios of 1:2:1.5 and calcined samples at 700°C are shown in Fig. 4.7. From the FTIR graph observed peaks can be found at 529, 682, 1384, 2291, 2349, 2375, 3496 cm⁻¹ wavenumber. The Mg-O-Al stretching vibration is responsible for the observed peaks in the 529 cm⁻¹ and 682 cm⁻¹ regions. The strong absorption band at 1384 cm⁻¹ can be referred to the presence of NO₃⁻ bending characteristic vibration. The C-N group vibration is responsible for the observed peaks in the range 2291 cm⁻¹, 2349 cm⁻¹, and 2375 cm⁻¹. Some are caused by bending, while others are caused by stretching. Due to bending vibration, a wavenumber of 2291 cm⁻¹ can be visible. Stretching vibration produces wavenumbers of 2349 and 2375 cm⁻¹. The bending vibration is responsible for the absorption band at 3496 cm⁻¹, which is caused by the OH group bending vibration. At 700°C, we can learn from FTIR analysis about diverse bonds such as O-H, Mg-O-Al, NO₃⁻ and so on.

4.4. FESEM OF MgAl₂O₄

4.4.1. FESEM OF MgAl₂O₄(Mg:Al:CA=1:2:1.5):

FESEM of calcined samples with Mg, Al, and citric acid molar ratios of 1:2:1.5 and calcined samples at 700⁰ C are shown in Fig. 4.8. From the figure we can get information about MgAl₂O₄ crystal structure.

1. **Flake Like structure**:-From the figure It can be clearly seen, flake like structure has been formed.
2. **Agglomerated Structure**:-From the figure it's clear that nanoparticles are stuck with each other and they form an agglomerated structure. The van der Waals forces, which cause the adhesion force between the particles, are the main cause of the agglomerates.
3. **Particle Size**:-From the photo It can be said that nanoparticles are about 20-25 nm size. They are in triagonal tetragonal or round in shape.

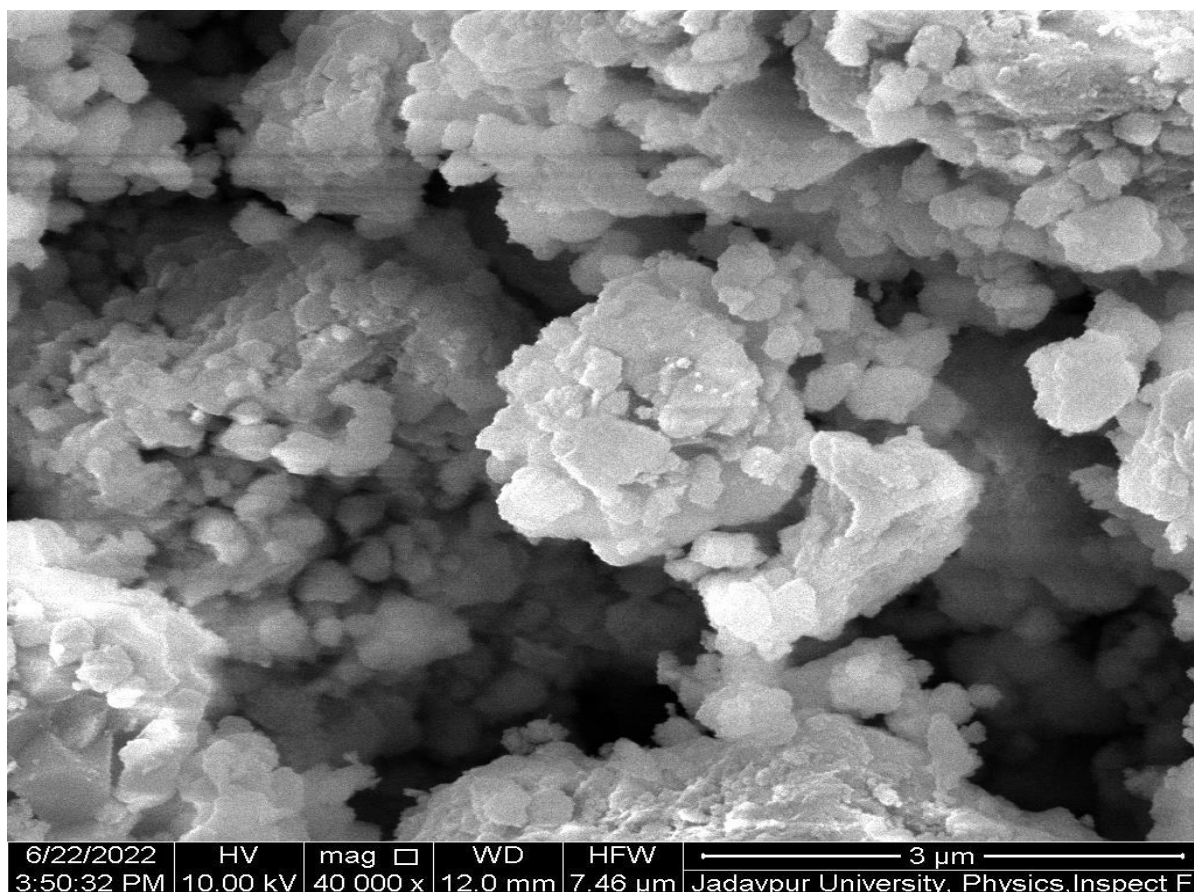


FIG-4.8- FESEM OF MgAl₂O₄(Mg:Al:CA=1:2:1.5)

4.4.2. FESEM OF $MgAl_2O_4$ (Mg:Al:CA=1:2:1.25):

FESEM of calcined samples with Mg, Al, and citric acid molar ratios of 1:2:1.25 and calcined samples at 700⁰ C are shown in Fig. 4.9. From the figure we can get information about $MgAl_2O_4$ crystal structure.

1. **Flake Like structure**:-From the figure It can be clearly seen, flake like structure has been formed.

2. **Agglomerated Structure**:-From the figure it's clear that nanoparticles are stuck with each other and they form an agglomerated structure. The van der Waals forces, which cause the adhesion force between the particles, are the main cause of the agglomerates.

3. **Particle Size**:-From the photo It can be said that nanoparticles are about 15-20 nm size. They are in triagonal tetragonal or round in shape. Particles are smaller in size than particle crystallized at 800⁰ C.

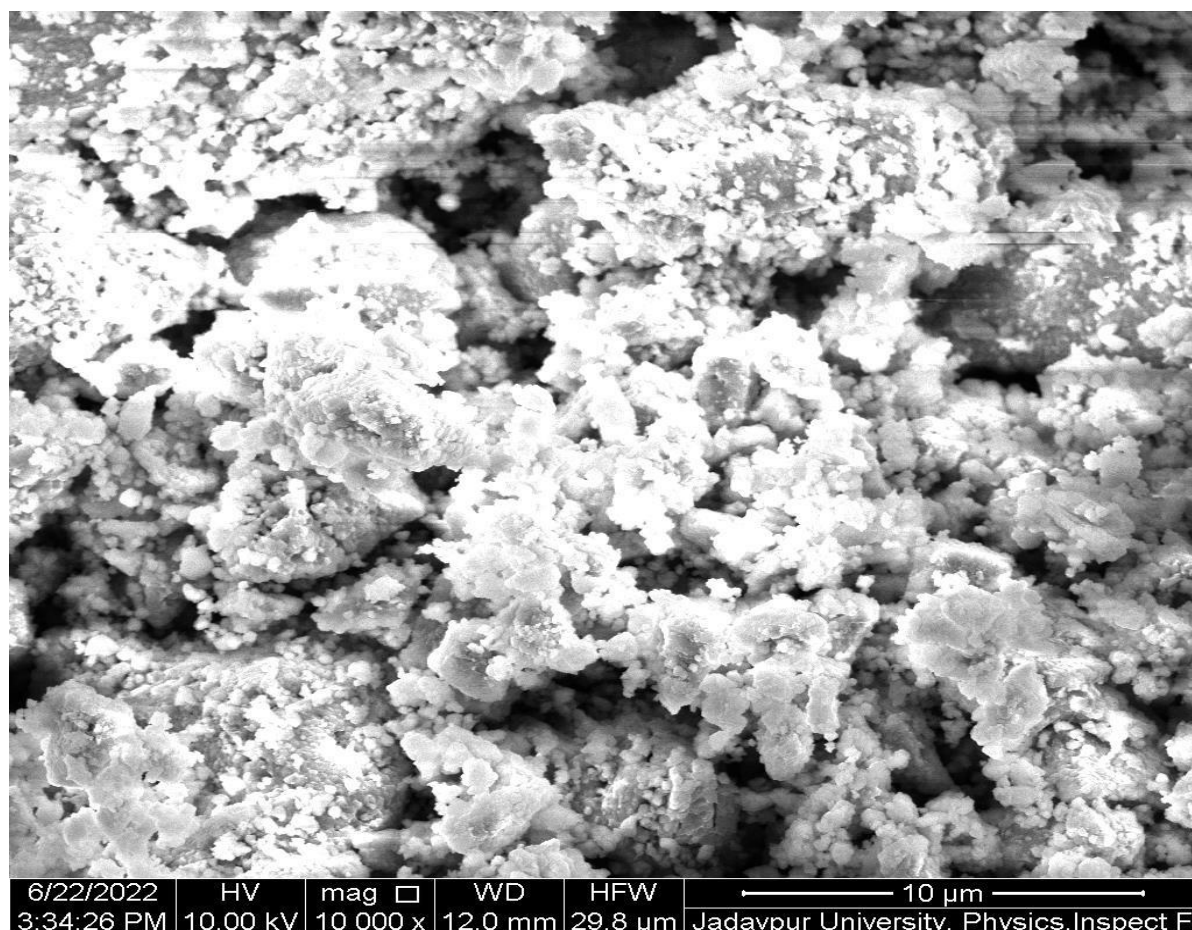


FIG-4.9- FESEM OF $MgAl_2O_4$ (Mg:Al:CA=1:2:1.25)

4.4.3. FESEM OF $MgAl_2O_4$ (Mg:Al:CA=1:2:1.25):

FESEM of calcined samples with Mg, Al, and citric acid molar ratios of 1:2:1.75 and calcined samples at $800^{\circ}C$ are shown in Fig. 4.10. From the figure we can get information about $MgAl_2O_4$ crystal structure.

1. **Flake Like structure**:-From the figure It can be clearly seen, flake like structure has been formed.

2. **Agglomerated Structure**:-From the figure it's clear that nanoparticles are stuck with each other and they form an agglomerated structure. The van der Waals forces, which cause the adhesion force between the particles, are the main cause of the agglomerates.

3. **Particle Size**:-From the photo It can be said that nanoparticles are about 10-15 nm size. They are in triangular tetragonal or round in shape. Particles are bigger in size than particle crystallized at $700^{\circ}C$.

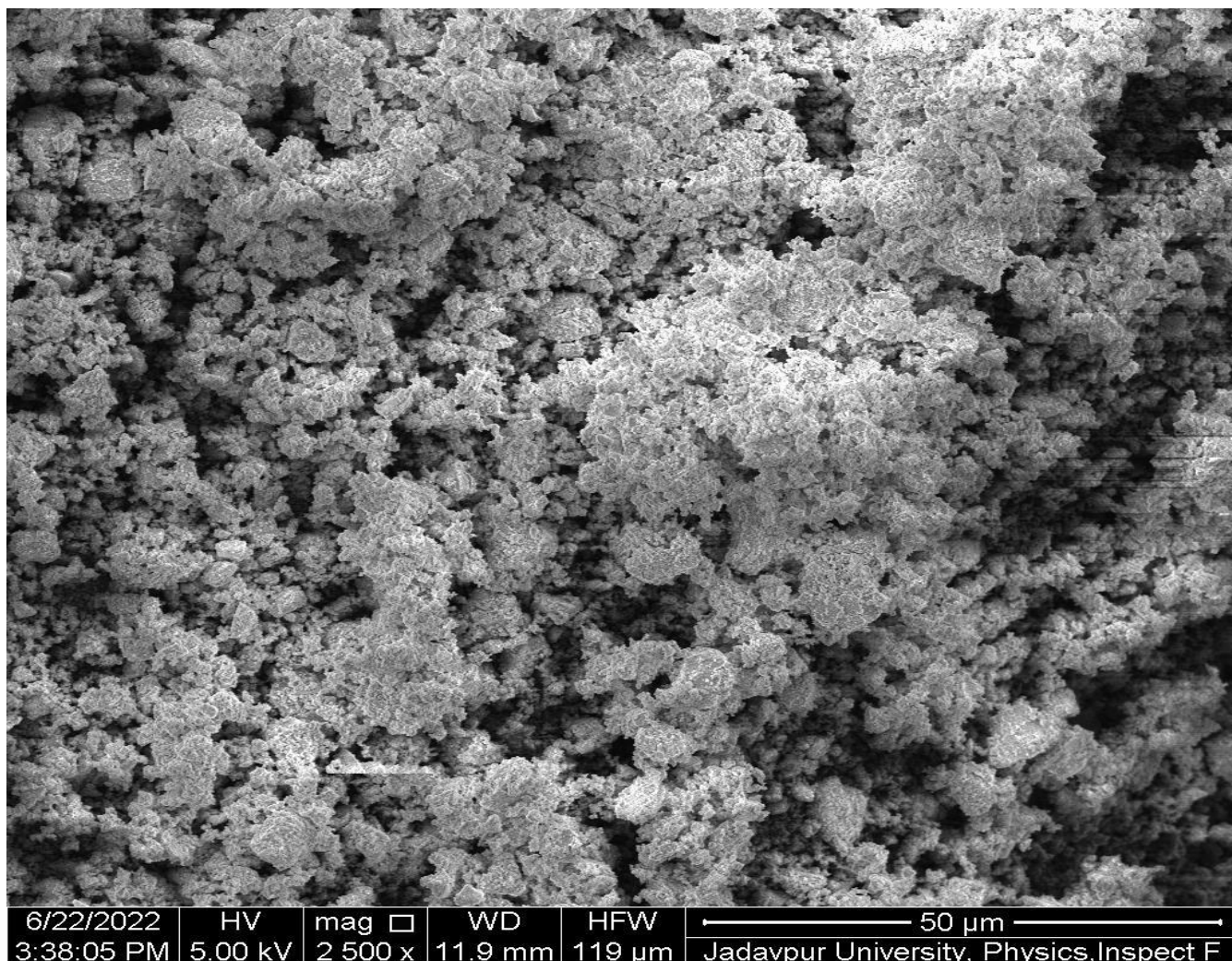


FIG-4.9- FESEM OF $MgAl_2O_4$ (Mg:Al:CA=1:2:1.25)

4.5. Micro-Hardnes of MgAl₂O₄:

Electronic micro hardness testing equipment is used to determine the micro hardness. Table 4.10 displays hardness values for each spinel composition.

Table-4.10

| Mg,Al,CA ratio of the sample(calcination temp.,time) | Microhardness(Gpa) |
|--|--------------------|
| 1:2:1.25(700 ⁰ C,6HR) | 7.69 |
| 1:2:1.25(700 ⁰ C,5 HR) | 6.89 |
| 1:2:1.25(700 ⁰ C,4 HR) | 7.39 |
| 1:2:1.5(800 ⁰ C,4 HR) | 8.64 |
| 1:2:1.5(800 ⁰ C,5 HR) | 8.54 |
| 1:2:1.5(800 ⁰ C,6 HR) | 8.88 |

Referring table 4.10 it can be observed that depending upon citric acid ratio, microhardness of the MgAl₂O₄ has increased.It can be observed that with Mg:Al:CA=1:2:1.25,average microhardness is 7.32 Gpa whereas with Mg:Al:CA=1:2:1.5,average microhardness is 8.68 Gpa. From this It can be said, with increasing citric acid ratio microhardness of the MgAl₂O₄ can be improved.

CHAPTER 5

CONCLUSION AND FUTURE SCOPE

CONCLUSION

For the MgAl_2O_4 spinel studies has been conducted by the synthesis using sol gel process using Magnesium Nitrate and Aluminium Nitrate as the precursor were used for the formation of MgAl_2O_4 . The homogeneous spinel with enhanced structural change is successfully synthesized by Molecular level mixing process and followed by Sintering. Pellets have been prepared from the white sintered powder by compressing. Microhardness of the prepared pellets has been studied. And the following conclusion can be drawn,

1. The sol-gel method was used to successfully manufacture nano-crystallite MgAl_2O_4 spinel powder.
2. The MgAl_2O_4 spinel powder's initial crystallisation temperature was 650°C . At 700°C degrees Celsius, pure MgAl_2O_4 spinel crystallised.
3. Cubic MgAl_2O_4 spinel phase has been produced at roughly 700°C without any separate impurity phase.
4. MgAl_2O_4 crystallite size was observed to be around 10 nm.

5. From the XRD

- It can be understood that at 650°C the spinel starts to crystallize, as a small peak can be found at 650°C for the sample.
- At 700°C crystallization of spinel occurs and 85.71% pure MgAl_2O_4 spinel has been crystallized. As from the XRD for Mg:Al:CA=1:2:1.75 6 peaks can be found out of which 5 peaks resemble MgAl_2O_4 and rest one resembles Al_2O_3 .
- At 800°C crystallization of spinel occurs and 85.71% pure MgAl_2O_4 spinel has been crystallized as from the XRD for Mg:Al:CA=1:2:1.5 for 6 hours 6 peaks can be found out of which 5 peaks resembles MgAl_2O_4 and rest one resembles Al_2O_3 .
- At 800°C crystallization of spinel occurs and 85.71% pure MgAl_2O_4 spinel has been crystallized as from the XRD for Mg:Al:CA=1:2:1.5 for 4 hrs calcination time 6 peaks could be found out of which 5 peaks resemble MgAl_2O_4 and rest one resembles Al_2O_3 .
- At 800°C crystallization of spinel occurs and 85.71% pure MgAl_2O_4 spinel has been crystallized as from the XRD for Mg:Al:CA=1:2:1.25 for 6 hrs calcination time 6 peaks can be found out of which 5 peaks resemble MgAl_2O_4 and rest one resembles Al_2O_3 .

6. From FTIR Analysis:

From FTIR graph we can say that there are stretching vibration of Al-O, Mg-O, Al-Mg bonds, which are discussed in previous FTIR explanation. So, it proves that we have MgO-Al₂O₃ system.

7. From FESEM Analysis:

From FESEM of calcined samples with different molar ratios of Mg, Al, and citric acid It can be said that flake Like, agglomerated Structure of MgAl₂O₄ has been formed with mean particle size 15-20 nm. The agglomerates are principally due to the adhesion force between the particles, which is induced by van der Waals forces. However, the agglomerates size in the sample at 800 °C is smaller than those observed in the sample at 700°C.

MICROHARDNESS:

From microhardness testing of MgAl₂O₄, It can be concluded that with increasing citric acid ratio microhardness of the MgAl₂O₄ can be improved.

FUTURE SCOPE:

- Taguchi modelling for optimization could be done with different parameters like calcination temperature, time, cost etc.
- Further research is necessary since the material is not entirely sintered in some ratios and the particles are not properly attached.
- It is necessary to research semiconductor properties.
- Future work will involve evaluating band gaps for optical research.

- Future work will involve employing transition metal ions as dopants for dielectric research.

CHAPTER 6

REFERENCES

- [1] Z. Szotek, W. M. Temmerman, D. Ködderitzsch, A. Svane, L. Petit, and H. Winter **“Electronic structures of normal and inverse spinel ferrites from first principles”**
- [2] “Crystal structural control on surface topology and crystal morphology of normal spinel (MgAl_2O_4)”, Journal of Crystal Growth 236 (2002) 441–454 by Dekkers R. and Woensdregt C.F.,
- [3] **“Corrosion-resistance of transparent ceramic spinel MgAl_2O_4 ”** by F. Wen, T.-Q. He, M.-Y. Lei, Q.-H. Song
- [4] **“Mechanical Properties and Thermal Shock Behaviour of Model $\text{MgO-MgAl}_2\text{O}_4$ Spinel Composite Refractories”** by Cemil Aksel, B. Rand, F.L. Riley.
- [5] **“Structural, electrical and dielectric properties of spinel type MgAl_2O_4 nanocrystallite ceramic particles synthesized by the gel-combustion method”** by Padmaraj Osaimany, Padmaraj Osaimany, N. Satyanarayana
- [6] “Properties of refractories” a book by Subrata Banerjee
- [7] **“Preparation and characterization of porous MgAl_2O_4 spinel ceramic supports from bauxite and magnesite”** by Feng Wang, Jianke Ye, Gang He, Guanghua Liu, Zhipeng Xie
- [8] “Refractory Materials, Metallurgical” by E. Ruh, in Concise Encyclopedia of Advanced Ceramic Materials, 1991
- [9] “THE THERMAL EXPANSION OF REFRACTORIES” by F. H. Norton
- [10] “Flexible and refractory tantalum carbide-carbon electrospun nanofibers with high modulus and electric conductivity” by Songzhi Zhou, Gangyong Zhou, Shaohua Jiang, Pinchao Fan, Haoqing Hou.
- [11] **W. H. Bragg: Philos. Mag.**, 1915, 30, (176), 305–315.
- [12] **S. Nishikawa: Proc. Math. Phys. Soc.**, 1915, 8, 199–209
- [13] Bhaduri S., Bhaduri S. B. and Prsbrey K. A., Journal of Material Research, 1999, 14, 3571–3580.

- [14] Bhaduri S. and Bhaduri S. B., *Ceramic International*, 2002, 28, 153–158.
- [15] Kanai T., Nakagawa Z., Ohya Y., Hasegawa M. and Hamano K.: Report RLEMTIT, 1987, 13, 75–83.
- [16] J. H. Belding and E. A. Letzgas: US Patent 3 950 504, 13 April 1976.
- [17] **M. O’Driscoll: *IM Fused Miner. Rev.*, 1997, (Spec. Iss.), 36–46.**
- [18] **“Formation and Densification Behavior of MgAl₂O₄ Spinel: The Influence of Processing Parameters”** by Ganesh Ibram, Susana M. Olhero, Avito Rebelo, José Ferreira.
- [19] “The Effect of Fine Alumina Type on Composition of in Situ Spinel Formation in Alumina-Magnesia Castables” By Ahmad Monshi, Masoumeh Paghandedh, Rahmatollah Emadi.
- [20] “Prediction of structure and cation ordering in an ordered normal-inverse double spinel” by Ghanshyam Pilania, Vancho Kocevski, J. A. Valdez, Cortney R. Kreller
- [21]] N. Hadian, M. Rezaei, Z. Mosayebi, F. Meshkani, CO₂ reforming of methane over nickel catalysts supported on nanocrystallite MgAl₂O₄ with high surface area, *J. Nat. Gas Chem.* 21 (2012) 200–206.
- [22] ZAMBONI L.A., CALIGARIS R.E. Different Compositions of MgO-C Bricks Used in Ladle Slag Line. In Proc. UNITECR’97. New Orleans, USA, 1997.
- [23] ANEZIRIS C.G., BORZOV D., ULBRICHT J. Magnesia Carbon Bricks-a High-Duty Refractory Material. *Interceram Refractories Manual*, 2003, pp. 22–27.
- [24] S. Mukhopadhyay, T.K. Pal, P.K. DasPoddar, “Improvement of corrosion resistance of spinel-bonded castables to converter slag” *Ceram. Inter.*, 35, pp. 373-380 (2009)
- [25] Lee, W.E., and Zhang, S., “Melt corrosion of oxide and oxide-carbon refractories”, *International Materials Reviews*, 44, pp.77-104 (1999).
- [26] Lee, W.E., and Zhang, S., “Direct and indirect slag corrosion of oxide and oxide-c refractories”, VII International Conference on Molten Slags Fluxes and Salts, The South African Institute of Mining and Metallurgy, pp.309-320 (2004).

- [27].Cooper, A.R., "Kinetics of refractory corrosion", *Ceramic Engineering and Science Proceedings*, 2, pp.1063-1086 (1982).
- [28] Taira, S., Nakashima, K., and Mori, K., "Kinetic behavior of dissolution of sintered alumina into CaO-SiO₂-Al₂O₃ slags", *ISIJ International*, 33, pp.116-123 (1993).
- [29] Gleiter, H., "Nanocrystallite materials: basic concept and microstructure", *Acta Mater.*, 48 (2000), pp.1-29;
- [30]. Tjong, S., and Chen, H., "Nanocrystallite materials and coatings", *Mater. Sic. Eng. Res.*, 45, pp.1-88 (2004).
- [31] GOTO K., LEE W. The "Direct Bond" in Magnesia Chromite and Magnesia Spinel. *Refractories. Journal of the American Ceramic Society*, Vol. 78, No. 7,
- [32] ANEZIRIS C.G., BORZOV D., ULBRICHT J. in " Magnesia Carbon Bricks-a High- Duty Refractory Material." In *Interceram Refractories Manual*, 2003, pp. 22–27.
- [33] ANAN K. Wear of Refractories in Basic Oxygen Furnaces (BOF). *Taikabutsu Overseas*, Vol. 21, No. 4, 2001, page no. 241-246.
- [34]E.N. Alvar, M. Rezaei, Mesoporous nanocrystallite MgAl₂O₄ spinel and its applications as support for Ni catalyst in dry reforming, *Scripta Mater* 360 (2009) 212–215
- [35]N. Hadian, M. Rezaei, Z. Mosayebi, F. Meshkani, CO₂ reforming of methane over nickel catalysts supported on nanocrystallite MgAl₂O₄ with high surface area, *J. Nat. Gas Chem.* 21 (2012) 200–206.
- [36]Z. Mosayebi, M. Rezaei, A.B. Ravandi, N. Hadian, Autothermal reforming of methane over nickel catalysts supported on nanocrystallite MgAl₂O₄ with high surface area, *Int. J. Hydrogen Energy* 37 (2012) 1236–1242.
- [37]C. Otero Areán, M. Peñarroya Mentrut, A.J. López López, J.B. Parra, High surface area nickel aluminate spinels prepared by a sol-gel method, *Colloid Surface A: Physicochem. Eng. Aspects* 180 (2001) 253–258.
- [38]S. Sanjabi, A. Obeydavi, Synthesis and characterization of nanocrystallite MgAl₂O₄ spinel via modified sol-gel method, *J. Alloys Compounds* 645 (2015) 535–540.

- [39] X.L. Pan, S.S. Sheng, G.X. Xiong, K.M. Fang, S. Tudyka, N. Stroh, H. Brunner, Mesoporous spinel MgAl₂O₄ prepared by in situ modification of boehmite sol particle surface: I Synthesis and characterization of the unsupported membranes, *Colloid Surfaces A: Physicochem. Eng. Aspects* 179 (2001) 163–169.
- [40] J. Tian, P. Tian, G. Ning, H. Pang, Q. Song, H. Cheng, H. Fang, Synthesis of porous 378 MgAl₂O₄ spinel and its superior performance for organic dye adsorption, *RSC Adv.* 5 (2015) 5123–5130.
- [41] P. Rao, R.C. Chikate, S. Bhagwat, Highly responsive and stable Y³⁺ dope
- [42]] J.-G. Li, T. Ikegami, J.-H. Lee, T. Mori, Fabrication of translucent magnesium aluminum spinel ceramics, *J. Am. Ceram. Soc.* 83 (2000) 2866–2868.
- [43] E.C. DeCanio, J.G. Weissman, FT-IR analysis of borate-promoted Ni-Mo/Al₂O₃ hydrotreating catalysts, *Colloid Surfaces A: Physicochem. Eng. Aspects* 105(1995) 123–132..
- [44] D. Schneider, D. Mehlhorn, P. Zeigermann, J. Karger, R. Valiullin, Transport properties of hierarchical micro-mesoporous materials, *Chem. Soc. Rev.* 45(2016) 3439–3467.
- [45] T. Shiono, K. Shiono, K. Miyamoto, G. Pezzotti, Synthesis and characterization of MgAl₂O₄ spinel precursor from a heterogeneous alkoxide solution containing fine MgO powder, *J. Am. Ceram. Soc.* 83 (2000) 235–237.
- [46] E.H. Walker Jr., J.W. Owens, M. Etienne, D. Walker, The novel low temperature synthesis of nanocrystallite MgAl₂O₄ spinel using “gel” precursors, *Mater. Res. Bull.* 37 (2002) 1041–1050.
- [47] Y. Suyama, A. Kato, Characterization and sintering of Mg-Al spinel prepared by spray-pyrolysis technique, *Ceram. Int.* 8 (1982) 17–21.
- [48] M.Y. Nassar, I.S. Ahmed, I. Samir, A novel synthetic route for magnesium aluminate (MgAl₂O₄) nanoparticles using sol–gel auto combustion method and their photocatalytic properties, *Spectrochim. Acta A* 131 (2014) 329–334.
- [49] E. Navaei Alvar, M. Rezaei, H. Navaei Alvar, H. Feyzallahzadeh, Z.-F. Yan, Synthesis of nanocrystallite MgAl₂O₄ spinel by using ethylene diamine as precipitation agent, *Chem. Eng. Commun.* 196 (2009) 1417–1424.
- [50] J. Chen, H. Arandiyani, X. Gao, J. Li, Recent advances in catalysts for methane combustion, *Catal. Surv. Asia* 19 (2015) 140–171.
- [51] S.A. El-Hakam, Structure, texture and catalytic activity of ZnO/Al₂O₃ catalysts, *Colloid Surfaces A: Physicochem. Eng. Aspects* 157 (1999) 157–166.

- [52] Y. Wang, H. Arandiyani, J. Scott, M. Akia, H. Dai, J. Deng, K.-F. Aguey-Zinsou, R. Amal, High performance Au–Pd supported on 3D hybrid strontium-substituted lanthanum manganite perovskite catalyst for methane combustion, *ACS Catal.* 412 (2016) 6935–6947.
- [53] , Edwin H Walker, Jr. Owens J W, Etienne M, et al. The novel low temperature synthesis of nanocrystallite MgAl₂O₄ spinel using “gel” precursors. *Materials Research Bulletin*, 2002, 37(6): 1041–1051.
- [54] I Ganesh , B Srinivas ,R Johnson “ Microwave assisted solid state reaction synthesis of MgAl₂O₄ spinel powders” in ‘*Journal of the European Ceramic Society*’ in 2004, 24(2): 201–207.
- [55] H. Reverón, *Mater. Lett.* 56, 97 (2002).
- [56] L.R. Ping, *Mater. Res. Bull.* 36, 1417 (2001).
- [57] Y. Wang, H. Arandiyani, J. Scott, M. Akia, H. Dai, J. Deng, K.-F. Aguey-Zinsou, R. Amal, High performance Au–Pd supported on 3D hybrid strontium-substituted lanthanum manganite perovskite catalyst for methane combustion, *ACS Catal.*(2016) 6935–6947.
- [58] Y. Wang, H. Dai, J. Deng, Y. Liu, H. Arandiyani, X. Li, B. Gao, S. Xie, 3DOM InVO₄- supported chromia with good performance for the visible-light-driven photodegradation of rhodamine B, *Solid State Sci.* 24 (2013) 62–70
- [59] H. Arandiyani, J. Scott, Y. Wang, H. Dai, H. Sun, R. Amal, Meso-molding three-dimensional macroporous perovskites: a new approach to generate high-performance nanohybrid catalysts, *ACS Appl. Mater. Interfaces* 8 (2016) 2457–2463.
- [60]] E. Yamamoto, K. Kuroda, Colloidal mesoporous silica nanoparticles, *Bull.Chem. Soc. Jpn.* 89 (2016) 501–539
- [61], G. Zhan, H.C. Zeng, Integrated nanocatalysts with mesoporous silica/silicate 423 and microporous MOF materials, *Coord. Chem. Rev.* 320–321 (2016) 181–192.

- [62], V. Malgras, Q. Ji, Y. Kamachi, T. Mori, F.-K. Shieh, K.C.-W. Wu, K. Ariga, Y. Yamauchi, Templated synthesis for nanoarchitected porous materials, *Bull. Chem. Soc. Jpn.* 88 (2015) 1171–1200.
- [63] K. Ji, H. Dai, J. Deng, H. Zang, H. Arandiyani, S. Xie, H. Yang, 3DOM BiVO₄ supported silver bromide and noble metals: high-performance photocatalysts for the visible-light-driven degradation of 4-chlorophenol, *Appl. Catal. B: Environ.* 168–169 (2015) 274–282
- [64] N. Majidian, N. Habibi, M. Rezaei, CH₄ reforming with CO₂ for syngas production over nickel catalysts supported on mesoporous nanostructured Al₂O₃, *Kor. J. Chem. Eng.* 31 (2014) 1162–1167. 434
- [65] J. Chen, W. Shi, X. Zhang, H. Arandiyani, D. Li, J. Li, Roles of Li⁺ and Zr⁴⁺ cations in the catalytic performances of Co₃Al_xM_xCr₂O₄ (M = Li, Zr; x = 0–0.2) for methane combustion, *Environ. Sci. Technol.* 45 (2011) 8491–8497. 437
- [66] H. Arandiyani, H. Dai, K. Ji, H. Sun, J. Li, Pt nanoparticles embedded in colloidal crystal template derived 3D ordered macroporous Ce_{0.6}Zr_{0.3}Y_{0.1}O₂: highly efficient catalysts for methane combustion, *ACS Catal.* 5 (2015) 1781–1793.
- [67] J. Akl, T. Ghaddar, A. Ghanem, H. El-Rassy, Cobalt ferrite aerogels by epoxide sol–gel addition: efficient catalysts for the hydrolysis of 4-nitrophenyl phosphate, *J. Mol. Catal. A: Chem.* 312 (2009) 18–22.
- [68] N. Habibi, H. Arandiyani, M. Rezaei, Mesoporous MgO—Al₂O₃ nanopowders supported meso-macroporous nickel catalysts: a new path to high-performance biogas reforming for syngas, *RSC Adv.* 6 (2016) 29576–29585.
- [69] Abdi, Md., Ebadzadeh, T., Ghaffari, A. and Feli, M., “Synthesis of nano-sized spinel (MgAl₂O₄) from short mechanochemically activated chloride precursors and its sintering behavior”, *Advanced Powder Technology*, 2014,

[70] Gilvan Per.de F., Alexander, F.M.C., Francisco M.S., Heloisa, Marcus and Dulce in "Synthesis of MgAl₂O₄ by Gelation Method: effect of Temperature and time of calcination in Crystallite Structure." July 6, 2017, ISSN 1980-5373

[71] Vahid B. R., Haghghi M., " Urea-nitrate combustion synthesis of MgO/MgAl₂O₄ nanocatalyst used in biodiesel production from sunflower oil: Influence of fuel ratio on catalytic properties and performance", Energy Conversion and Management 126 (2016) 362–372

[72] Viacheslav S., Marina K., Vladimir S., Semen K., Kirill M., Ivan P. and Vasiliy D. in "Preparation of Periclase-Magnesium Aluminate Spinel Ceramics from raw amorphous Magnesite and Aluminium Oxide Nanopowders", Oct 14th – 16th 2015, Brno, Czech Republic, EU, RFMEFI594144X0010.

[73] Li Hui, WEI H. Y., Cui Y., Sang Rong-Li, Bu Jing-Long, Wei Ying-Na, Lin Jian and Zhao J.H. in "Synthesis and characterisation of MgAl₂O₄ spinel nanopowders via nonhydrolytic sol-gel route", Journal of the Ceramic Society of Japan 125 [3] 100-104 2017

[74] Ibram Ganesh, Susana M. O., Avito H. Rebelo, and Ferreira J. M. F. in "Formation and Densification Behavior of MgAl₂O₄ Spinel: The Influence of Processing Parameters", Journal of American Ceramic Society, 91 [6] 1905–1911 (2008).

[75] Padmaraja O., Venkateswarlu M. and Satyanarayana N. in "Structural, electrical and dielectric properties of spinel type MgAl₂O₄ nanocrystallite ceramic particles synthesized by the gel-combustion method". Ceramics International 41(2015)3178–3185.

[76] Golyeva E.V., Kolesnikov I.E., Lahderantad E., Kurochkinc A.V. and Mikhailovb M.D. in "Effect of synthesis conditions on structural, morphological and luminescence Properties of MgAl₂O₄:Eu³⁺ nanopowders", Journal of Luminescence 194 (2018) 387–393.

[77] Miroliaee A., Salehirad A. and Rezvani A. R. in "Ion-pair complex precursor approach to fabricate high surface area nanopowders of MgAl₂O₄ spinel", Materials Chemistry and Physics xxx (2014) 1-6.

[78] Sanjabi S. and Obeydavi A. in "Synthesis and characterization of nanocrystallite MgAl₂O₄ spinel via modified sol-gel method". Journal of Alloys and Compounds JALCOM 34223

[79] Rahmat N., Yaakob Z., Pudukudy M., Rahman N. A. and Jahaya S. S. in "Single step solid-state fusion for MgAl₂O₄ spinel synthesis and its influence on the structural and textural properties". Powder Technology PTEC 13183.

[80] Synthesis And Characterization of Spinel (MgAl₂O₄) Using Sol- Gel Technique Prasad Ram Chavan¹ M. Senthil Kumar²

